1

Open-Shell Benzenoid Polycyclic Hydrocarbons

Soumyajit Das and Jishan Wu

1.1

Introduction

Graphene has been found to be an attractive material since its discovery in 2004 and has drawn enormous interest among researchers owing to its intrinsic electronic and magnetic properties. An indefinitely large graphene sheet, if cut along the two edge directions, can generate two distinct, well-defined small graphene nanoribbons (GNRs), which may be classified into "zigzag" edge (**1**, *trans*-polyacetylene) and "armchair" edge (**2**, *cis*-polyacetylene) structures (Figure 1.1). If graphene is cut in an all-zigzag fashion or in a triangular shape, the smallest unit that would come out is a phenalene unit (**3**) with one unpaired electron. The larger frameworks when cut in a zigzag shape will indefinitely lead to a series of non-Kekulé (i.e., open-shell) polycyclic hydrocarbons (PHs, **4**–**6**) possessing one or more unpaired electrons, which can be termed as "open-shell graphene fragments" and are very interesting in terms of academic research. The number of unpaired electrons, or radicals, increases with the size of the framework, starting from phenalenyl monoradical to high-spin polyradical systems (**3**–**6**, Figure 1.1). If a graphene sheet is cut in an all-armchair fashion, it would lead to "all-benzenoid PHs," as their structures can be represented as fully aromatic sextet rings (the six-membered rings highlighted in blue background) without additional double bonds (**7**). Even though the PHs of such category are larger in size with extended conjugation, they generally show high stability due to the stabilization through the existence of more number of Clar's aromatic sextets (**8**). The studies on hexa-*peri*-hexabenzocoronene and other extended all-benzenoid PHs have provided information on armchair-edged GNRs at the molecular level [1].

Another intriguing class of PHs would be rectangular-shaped GNRs, which are characterized by existence of both zigzag and armchair edges (**9**, Figure 1.1) with a typical Kekulé (i.e., closed-shell) structure. Their structures can be formulated by cycles in a monocyclic system symbolizing benzenoid aromatic sextet rings according to Clar's aromatic sextet rule [2]. Therefore, the more Clar's sextets the molecule can have, the more stable the system will be. Interestingly, recent theoretical and experimental work indicate that for rectangular PHs with extended

Polycyclic Arenes and Heteroarenes: Synthesis, Properties, and Applications, First Edition. Edited by Qian Miao.

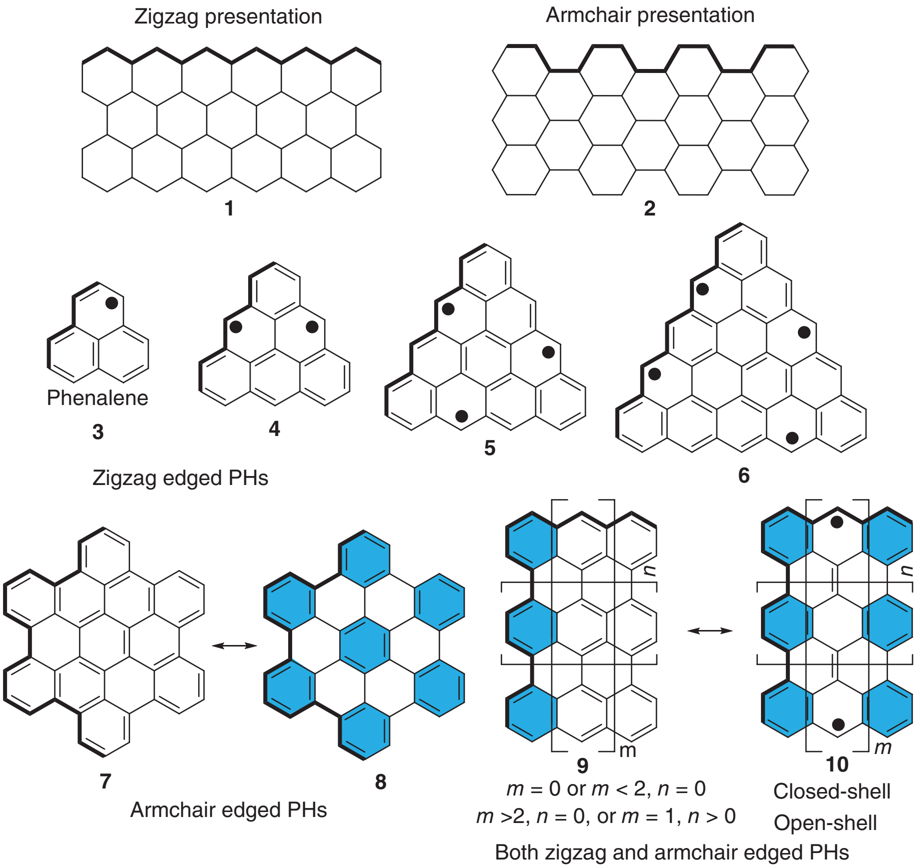

Figure 1.1 Molecular graphenes by fusion of benzene rings in different modes.

zigzag edges, such as anthenes and periacenes, a remarkable open-shell diradical character will emerge when the conjugation is extended to a certain point ($n > 0$ for anthenes and $m > 2$ for periacenes), which originates from a narrowed bandgap and stabilization through more Clar's sextet rings in the diradical form (**10**, Figure 1.1). The molecule possesses more aromatic sextet rings in the diradical or poly-radical resonance forms and, if the recovered resonance energy can compensate the energy required to break a double bond, an open-shell singlet diradical or polyradical ground state could appear. Two very nice examples to validate such a statement are the teranthene and quarteranthene derivatives reported by Kubo *et al.*, which will be discussed in following sections.

Most benzenoid PHs actually can be characterized by a closed-shell electronic configuration accommodating their π electrons only in bonding orbitals. However, researchers faced difficulties for certain types of PHs due to their high reactivity. An important work by Bendikov *et al.* came into spotlight in 2004 when their computational study on oligoacenes supported that the longer acenes possessed a nonzero bandgap with a singlet open-shell ground state followed by a higher energy triplet state [3]. The open-shell electronic configuration refers to the existence of one or more unpaired electrons, or radicals, in the molecular structure [4]. The electronic states of the open-shell systems with two unpaired electrons can be further divided into open-shell singlet, when the unpaired electrons adopt antiparallel spin, or open-shell triplet, when the unpaired electrons adopt parallel spin. Among all of the electronic states, the one with the lowest energy defines the ground state of π-conjugated systems. The high reactivity derived from open-shell nature of these systems in the ground state largely impedes their synthesis and isolation, but still continuous efforts have been made to synthesize and stabilize them due to the passion to understand the interplay of the unpaired electrons and delocalized π-electron systems and charge fluctuation, as well as the possibility of using them as molecule-based functional materials [5]. Therefore, the ground state can now be systematically studied by various spectroscopic techniques including nuclear magnetic resonance (NMR), electron spin resonance (ESR), ultraviolet–visible–near infrared spectroscopy (UV–vis–NIR), Raman spectroscopy, X-ray crystallographic analysis, and superconducting quantum interfering device (SQUID) measurements, assisted by density functional theory (DFT) calculations.

Theoretically, the diradical character (y) ($0 < y < 1$, where $0 =$ closed-shell, $1 =$ open-shell) can be estimated by the extent of the mixing of highest occupied molecular orbital (HOMO) and lowest unoccupied molecular orbital (LUMO) in the ground state [6]. The occupation number of the LUMO is used as an index of the diradical character, which can be estimated by a complete active space self-consistent field (CASSCF) calculation using the restricted Hartree–Fock (RHF) and two-configuration self-consistent field (SCF) calculations considering the Coulombic interaction between two unpaired electrons permitted to occupy the different parts is space. Another approach [7] is the broken-symmetry (BS) formalism based on the unrestricted Hartree–Fock (UHF) wave function, which defines the occupation number of the lowest unoccupied natural orbital (LUNO) as the extent of the diradical character [8]. This method was further revised by applying a spin-projection method to discard the spin contamination problem [9]. The diradical character can be also evaluated experimentally using the following formula [10], recently proposed by Kamada *et al.*:

$$y = 1 - \sqrt{1 - \left(\frac{E_{S1u,S1g} - E_{T1u,\ S1g}}{E_{S2g,S1g}}\right)^2}$$

where E_{S1u}'$_{S1g}$ and $E_{S2g,S1g}$ correspond to the energy of the lowest energy peaks in the one- and two-photon absorption (TPA) spectra, and $E_{T1u,S1g}$ corresponds to the energy gap between the triplet and the singlet ground state.

The synthesis and study of open-shell PHs have become a rising hot topic nowadays, so we aim to provide a brief overview on recent advancements including theoretical studies and experimental characterizations of a series of benzenoid PH-based diradicaloids comprising higher order acenes, bis(phenalenyl)s, zethrenes, anthenes, and periacenes, π-extended *p*-quinodimethane, and triangulene-based triplet biradicals.

1.2
Higher Order Acenes

Acenes can be regarded as one-dimensional fragments of graphene and belong to a class of PHs consisting of linearly fused benzene rings. The small acenes, namely naphthalene and anthracene, are among the most widely studied organic molecules, while the fascinating electronic properties of pentacene and higher order acenes larger than pentacene [11] have received considerable attention [12]. Pentacene has a closed-shell singlet (CS) ground state and has been the center of attention among the materials scientists as an effective organic semiconducting material in organic field-effect transistors (OFETs) because of its potentially high charge-carrier mobility. Synthesis of acenes larger than pentacene is, however, hampered by their increased reactivity as the number of rings increases [13]. Significant efforts had been devoted to the development of appropriate methods, albeit tedious, for the synthesis of larger stable acenes, which was quite challenging because of their very low solubility, poor light and oxygen stability, and their tendency to dimerize [14]. Despite of challenges, noteworthy progress has been made in the synthesis of larger acenes in recent years. The electronic properties, aromaticity, and HOMO–LUMO gaps of larger acenes have been examined extensively using computational techniques [12a], but we will be highlighting their “open-shell” characteristics.

The open-shell feature of acenes can be symbolized by the chemical structure of acenes (as exemplified by pentacene **11** in Figure 1.2) in either a closed-shell Kekulé form (**11**) with only one aromatic sextet ring, or a diradical (**17a**)/tetraradical (**17b**) form with two or three aromatic sextet rings. The extra aromatic rings can help to compensate the energy loss from π-bond cleavage and enhance the open-shell contribution to the ground state. Studies have revealed that linear oligoacenes possess the CS ground state, and only those larger than hexacene are expected to have open-shell diradical character in their ground states but these are still not completely understood and a large controversy was

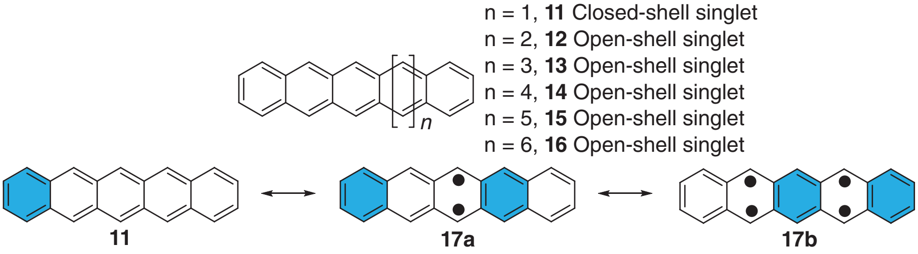

Figure 1.2 Resonance forms of pentacene **11**.

raised from the ground-state multiplicities of larger oligoacenes. Calculations on the ground state of higher order acenes by Angliker *et al.*, by the extrapolation of experimental singlet–triplet differences from benzene to hexacene, indicate a triplet ground state from nonacene onwards, although no actual triplet relative energy was determined [15]. Houk *et al.*, on the basis of B3LYP calculations, proposed that the higher order acenes above nonacene could be treated as two parallel polyacetylene ribbons with a triplet ground state and a vanishing bandgap [16]. These results were later challenged by Bendikov *et al.*, who theoretically investigated the open-shell diradical character of oligoacenes, namely, hexacene (**12**), heptacene (**13**), octacene (**14**), nonacene (**15**), and decacene (**16**) (Figure 1.2). They found that the wave function at the RB3LYP/6-31G(d) level of theory became unstable for oligoacenes larger than hexacene, while reoptimization using the unrestricted broken symmetry B3LYP method (UB3LYP) led to a singlet state with diradical character as a consequence of the disjoint nature of ground states of oligoacenes. Calculations on open-shell singlet (S), triplet (T), and CS states were found to be $\Delta E_{\mathrm{S-T}} = -10.3\,\mathrm{kcal\,mol^{-1}}$ and $\Delta E_{\mathrm{S-CS}} = -0.8\,\mathrm{kcal\,mol^{-1}}$, clearly revealing that the open-shell singlet state is lower in energy than the triplet and CS states, respectively, for hexacene. The open-shell singlet to triplet energy gap for hexacene to heptacene and octacene follows a decreasing trend before eventually becoming constant at nearly $-5.5\,\mathrm{kcal\,mol^{-1}}$. The open-shell singlet to CS state energy also follows a similar trend from -0.8 to $-10.4\,\mathrm{kcal\,mol^{-1}}$; however, no saturation point is reached. The calculated frontier molecular orbital profiles further clarified the disjointed character of the diradical, indicating the singlet ground state. A detailed investigation was documented by Hachmann *et al.* up to dodecacene using CASSCF calculations in the framework of a density matrix renormalization group (DMRG) algorithm. Apart from the open-shell singlet ground state envisaged for larger oligoacenes, acenes larger than dodecacene were found to exhibit a singlet polyradical character in their ground state having one unpaired spin with every five to six rings [17]. Jiang *et al.* further supported Hachmann's claim by using a spin-polarized DFT method on oligoacenes up to 40 acenes [18], and a valence bond study by Qu *et al.* utilizing the DMRG technique confirmed the open-shell polyradical nature of oligoacenes in the ground state [19].

In spite of the myriads of theoretical results, experimental results on higher order acenes are scarce because of several factors including tedious synthetic procedure, high-lying HOMO [20], open-shell character that makes the oligoacenes vulnerable to dimerization [21] or polymerization [14], Diels–Alder reactions with oxygen [13a], as well as nucleophilic and electrophilic additions [13b]. The most salient experimental features of a PH with an open-shell singlet diradical ground state include the line broadening of ^{1}H NMR spectrum arising from the existence of thermally excited triplet species, and the observation of a featured electronic absorption band associated with a doubly excited electronic configuration in the ground state. The hexacene and heptacene derivatives reported so far are quite reactive [22], which may support the open-shell singlet diradical character in the ground state [3]. However, this is not detectable spectroscopically (^{1}H NMR signals show sharp splitting and narrow line widths indicating a closed-shell ground state). It is worth mentioning that a physical vapor-transport method was recently introduced to generate platelet-shaped crystals of hexacene by thermal degradation of its monoketone precursor. The hexacene thus obtained was found to be remarkably stable under ambient conditions in the dark [23]. Nevertheless, the preliminary reports provided valuable information that trialkylsilylethynyl groups, whose diameter is approximately 35–50% of the length of heptacene, provide sufficient protection through steric effects to exert a significant stabilizing effect [22a]. This observation made a major impact in the evolution of stable higher order acenes up to nonacene.

The synthesis and spectroscopic detection of unsubstituted octacene and nonacene was reported by Bettinger's group by using a cryogenic matrix-isolation technique [24]. The approach relies upon a protecting-group strategy based on the photochemically induced bisdecarbonylation of bridged diketones (Figure 1.3). The removal of diketone bridges in tetraketone precursors **18** by UV irradiation under matrix-isolation conditions can afford unsubstituted octacene and nonacene **19** detectable with UV–vis–NIR. The first ever fully characterized "persistent" nonacene derivative was reported by Miller and coworkers [25]. The key step involved the Diels–Alder reaction of arylthio-substituted 1,4-anthracene quinone **20** with bis-*o*-bromodimethane precursor **21** to produce a nonacene skeleton in the form of diquinone **22**. Nucleophilic addition on **22** with aryl lithium reagent followed by reduction/aromatization gave the substituted nonacene **23**. Despite the narrow HOMO–LUMO gap (1.12 eV), which is the smallest experimentally measured energy gap for any acene, the nonacene derivative **23** is stable as a solid in the dark for at least 6 weeks because of the closed-shell electronic configuration resulting from arylthio substituent effects, and it was fully characterized by a suite of solution-phase techniques, including sharp ^{1}H NMR, ^{13}C NMR, UV–vis–NIR, laser-desorption mass spectroscopy, and fluorescence spectroscopy. However, Miller also proposed an open-shell singlet diradical ground state for this nonacene by unrestricted broken spin-symmetry DFT (UBS-DFT) at B3LYP/6-31G*, irrespective of the positions of the substituents [26]. On the other hand, Anthony *et al.* reported new nonacene derivatives protected by trialkylsilylethynyl and bis(trifluoromethyl)phenyl groups on the zigzag edges and fluorine atoms at both the outer phenyl rings [27]. The synthesis of **26** was straightforward, and involved the alkynylation of the quinone **24** followed by re-aromatization of the corresponding tetra-ols **25** and **26**. The nonacene **26** showed a prominent S_0–S_1 transition at 1014 nm but only weak absorptions throughout the visible region with a low HOMO–LUMO gap of 1.2 eV. All three nonacene derivatives reported by Anthony's group were unambiguously characterized by single-crystal analysis and shown to be packed as perpendicular one-dimensional (1D) "slipped" stacks. Interestingly, the absence of an NMR signal and presence of an ESR signal with $g = 2.0060$ for the nonacene sample (**26**, R = –*i*Bu) (Figure 1.3) could be an intrinsic trait of its open-shell nature, which however was not confirmed.

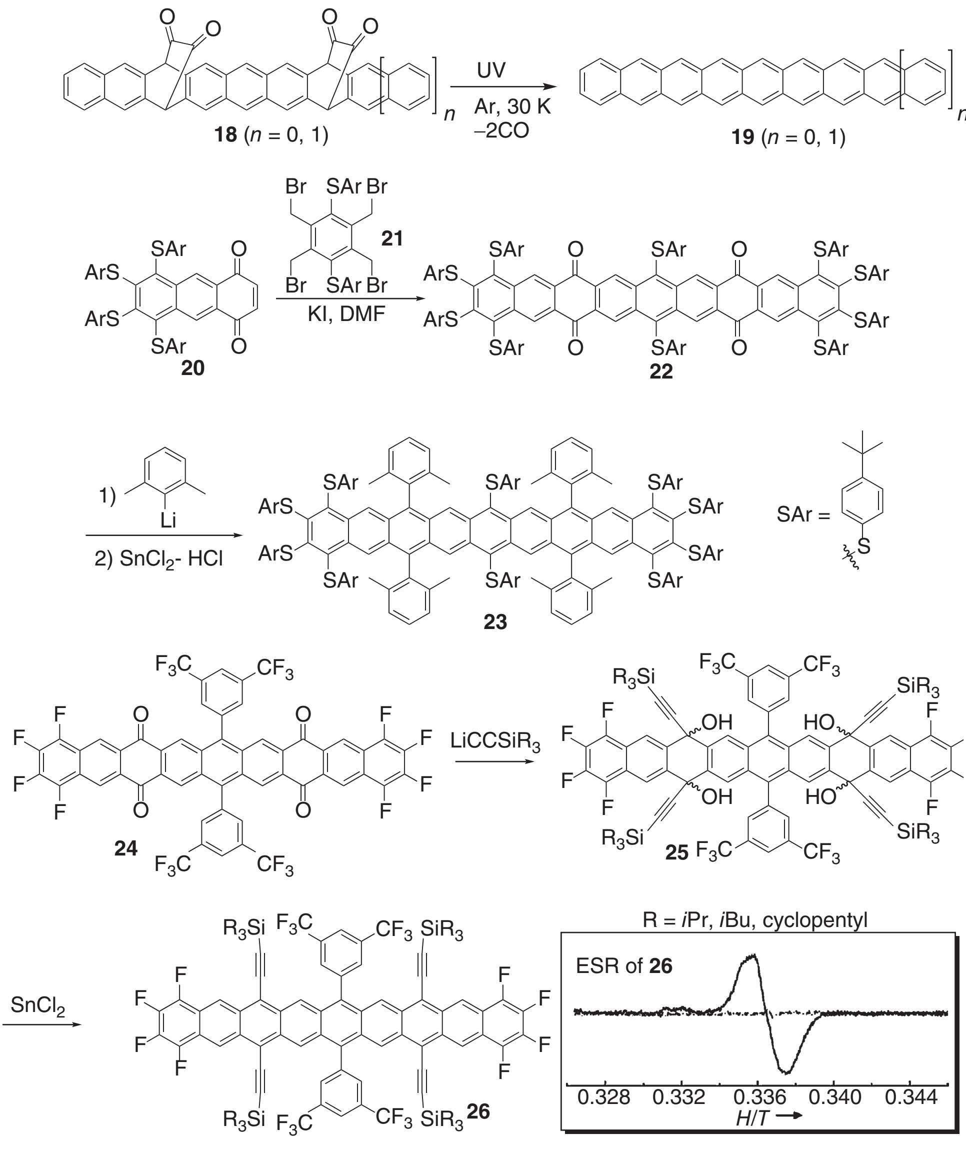

Figure 1.3 Nonacene derivatives. (ESR spectra of **26** is adapted with permission from Ref. [27]. Copyright 2011, John Wiley and Sons.)

1.3
Phenalenyl-Based Diradicaloids

The phenalenyl moiety is composed of a triangular fusion of three benzene rings where three C–C bonds are shared between the rings (Figure 1.1) and contains an uneven number of carbon atoms and, hence, in its neutral state, an uneven number of electrons or a radical. Phenalenyl derivatives can thus be regarded as "open-shell graphene fragments" and have been of central interest in both basic science and materials science [28]. The research on phenalenyls could lead to a better understanding of the intriguing electronic and magnetic properties of nanographene [29]. Since the studies on the phenalenyl-based monoradicals have been well reviewed by Morita and Nishida [5], here we highlight only the research work on the phenalenyl-based diradicaloid systems.

1.3.1
Bis(phenalenyl)s

The design strategy for bis(phenalenyl)-based diradicaloids is to link two phenalenyl moieties with an aromatic bridge to produce open-shell systems with a Kekulé resonance structure. These systems were first studied by Nakasuji and Kubo [30]. Two factors play a major role in stabilization of these systems: one is the intrinsic delocalization of phenalenyl moiety, and the other is the aromatic stabilization through the recovery of one additional aromatic sextet ring from the quinoidal resonance form to the diradical resonance form. Pentalenodiphenalene (PDPL, **27**) [31], the first member of this family, was reported in 1983 (Figure 1.4) and showed interesting amphoteric multistage redox properties, although its neutral state was substantially destabilized by the electronic contribution from 8π-electron antiaromatic pentalene subunit. Subsequently, indacenodiphenalene (IDPL, **28a**) with one benzene ring fused in the center was developed, and various substituents were introduced to improve the solubility [32]. These compounds were featured by a singlet diradical ground state. The line broadening in the ^{1}H NMR spectra at elevated temperature as well as the emergence of sharp peaks at lower temperature, together with solid-state ESR peaks, clearly indicated a thermally accessible triplet species at room temperature. The energy separation between the ground singlet state and the excited triplet state was further determined as $20.4 \pm 0.3\,\mathrm{kJ\,mol^{-1}}$. The crystal structure of **28d** demonstrated 1D chains in staggered stacking mode with an average π–π distance of 3.137 Å, which is significantly shorter than the Van der Waals contact of the carbon atoms (3.4 Å). This packing mode will maximize the SOMO–SOMO (singly occupied molecular orbital) overlap between the radicals, leading to stabilized intermolecular orbitals corresponding to intermolecular covalency [33]. A naphthalene-linked bis(phenalenyl) compound **29a** with larger diradical character than **28** was synthesized by Kubo *et al.* [34]. The electrochemical HOMO–LUMO gap was determined as 1.04 eV, and the singlet–triplet gap ($\Delta E_{\mathrm{S-T}}$) was estimated to be 1900 K by SQUID measurements, both being smaller than those of **28d** (1.15 eV and $\Delta E_{\mathrm{S-T}} = 2200\,\mathrm{K}$), thereby supporting its larger diradical character. The packing of **29b** adopted a similar stepped mode as **28d** in the 1D chain, and the intermolecular bonding was stronger than the intramolecular one due to the spin-localized nature on the phenalenyl moieties, which can be more adequately described as multicenter bonding. Bis(phenalenyl)s linked by anthracene unit **30** was also synthesized by the same group [35] and was reported to have a larger diradical contribution ($y = 0.68$) compared to its naphthalene ($y = 0.50$)

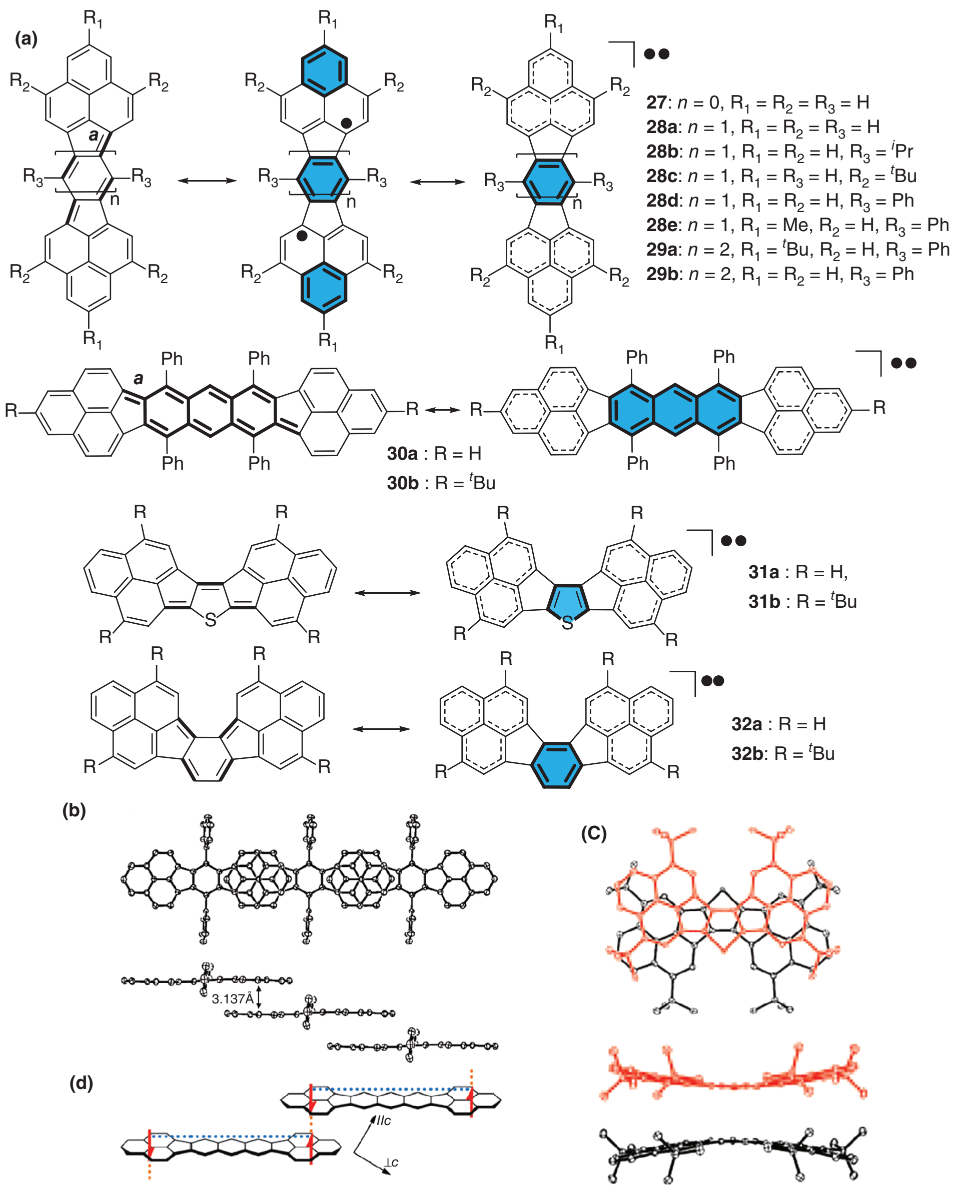

Figure 1.4 (a) Resonance forms of bis(phenalenyls) with different aromatic linkers. (b) Crystal structure of **28d**. (Adapted with permission from Ref. [33]. Copyright 2005, John Wiley and Sons.) (c) Crystal structure of **31b**. (Adapted with permission from Ref. [36]. Copyright 2004, John Wiley and Sons.) (d) Intra and intermolecular covalent bonding interactions in a schematic 1D stack of **30a** (blue and orange dotted lines). (Adapted with permission from Ref. [35]. Copyright 2012, Royal Society of Chemistry.)

and benzene ($y = 0.30$) counterparts, in the ground state. The enhanced diradical contribution of **30** was further supported by X-ray crystallographic analysis, where the bond *a* in **30b** was found to be more elongated (1.467(3) Å) compared to that of **29a** (1.465(7) Å) and **28e** (1.457(2) Å); a similar intermolecular covalent bonding interaction with a distance of 3.122 Å between the molecules in a 1D chain was observed. The transition moment in the 1D stack of **30a** is tilted to the perpendicular direction (the orange dotted line direction) with respect to the line connecting the centers of gravity of the molecule. This finding experimentally demonstrates that the covalent bonding interaction in the 1D stack of **30a** is considerably stronger between molecules compared to that within a molecule. The significant diradical contribution of **30** was attributed to the high aromatic stabilization energy of the anthracene linker. A thiophene unit, instead of phenyl/naphthalene/anthracene linker, was also used to bridge two phenalenyl systems. The thiophene fused bis(phenalenyl) **31** showed amphoteric redox property with a small HOMO−LUMO gap. The diradical character index *y* was estimated to be 0.35, and DFT calculation at UB3LYP/6-31G(d,p) level predicted a singlet diradical ground state that is stabilized by 7 kJ mol^{-1} more than that of singlet closed-shell state. X-ray crystallographic analysis revealed two kinds of dimeric pairs with substantially short nonbonding contacts of about 3.1 Å between each thiophene ring [36]. Accommodation of a doubly excited configuration in the ground-state stabilized this system by suppressing the four-electron repulsion arising from the interaction between fully occupied orbitals. Fusion of phenalenyl to the ortho positions of the phenyl ring led to compounds **32a** and **32b**, the latter with *tert*-butyl substituents being reported to be extremely air-sensitive and decompose in the air compared to **28c** which was stable for several weeks [37]. ^{1}H NMR spectra gave no useful information about the structure of **32b** because of the absence of signals in the aromatic regions at room temperature and broadened peaks at low temperature. However, dissolution of **32b** in D_2SO_4 gave clear spectra assignable to signals of the dicationic species **32b**$^{2+}$, thereby supporting the formation of **32b**. An energy lowering of 35.38 kJ mol^{-1} from the singlet closed-shell form to the singlet open-shell form was calculated for **32a**, suggesting its singlet diradical ground state [38].

Two bis(phenalenyl)s-based stable monoradicals are worth mentioning here. Bis(phenalenyl)s linked through a five-membered ring to produce a monoradical system **33a** was synthesized by Kubo *et al.* [39]. The resonance structures of this molecule indicated a fully delocalized radical among this molecule exerting high stabilization even in absence of any steric protection (Figure 1.5a). An evenly distributed spin density throughout the whole molecular backbone was theoretically predicted using the UBLYP/6-31G**//UB3LYP/6-31G** method. The extensive delocalization of unpaired electron also suppressed the formation of the σ-dimer as evident from the unchanged multiline ESR signal intensity from room temperature to −90 °C. The butyl-substituted compound **33b** was also prepared to increase the solubility and to obtain a single crystal. X-ray crystallographic analysis indicated the formation of π dimers in the solid state (Figure 1.5b) with multicenter bonding, and the strength of antiferromagnetic coupling ($2J/k_B$)

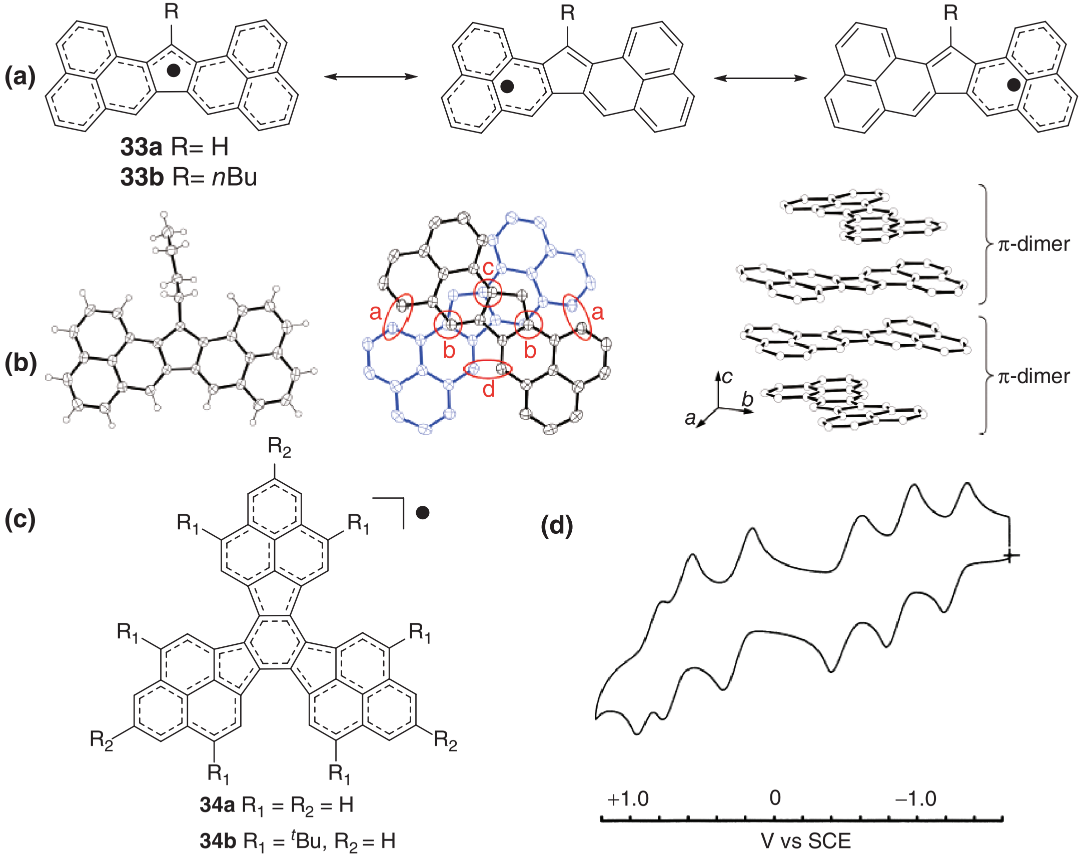

Figure 1.5 (a) Resonance structures of radical **33**. (b) Single-crystal structures of **33b**. (Adapted with permission from Ref. [39]. Copyright 2011, American Chemical Society.) (c) Structure of trisphenalenyl radical **34**. (d) Cyclic voltammogram of **34b**. (Adapted with permission from Ref. [6]. Copyright 2014, John Wiley and Sons.)

was determined by SQUID measurements as −1600 K within the π-dimer, which would split the SOMO of **33b** into bonding and antibonding molecular orbitals within the π-dimer. The half-life in air determined at room temperature was almost 60 h, which is in contrast to the rapid reaction of the phenalenyl radical with oxygen, suggesting that spin delocalization is very effective for the stabilization of organic radicals. Fusion of three phenalenyl units onto one benzene ring was supposed to lead to a highly delocalized monoradical system, but the very low solubility of the synthetic intermediates and, furthermore, the oxygen-sensitive trihydro precursor of **34a** hampered the characterization of the desired oxidized product (Figure 1.5c) [40]. *tert*-Butyl groups were then introduced to improve the solubility and stability, and subsequent reactions eventually gave rise to a hexa-*tert*-butyl derivative **34b**, which showed a nice redox amphotericity [6]. The neutral radical gave six reversible one-electron redox waves (Figure 1.5d), providing evidence for the formation of stable mono-, di-, and trivalent species, making **34b** one of the rare example of compounds with six-stage amphoteric redox behavior.

1.3.2
Zethrenes

A “head-to-head” fusion of two phenalenyl moieties will generate a “Z” shaped aromatic hydrocarbon called “zethrene,” which was first reported by Clar [41] (Figure 1.6). It can be regarded as a PH in which two naphthalene units are fixed by a *trans*-1,3-butadiene unit (Figure 1.6, $n = 0$). Extension of the butadiene unit gives higher order zethrene analogs such as heptazethrene (**35a**, $n = 1$) and octazethrene (**35b**, $n = 2$), in which two naphthalene units are bridged by a *para*-quinodimethane (*p*-QDM) and 2,6-naphthoquinodimethane unit, respectively. The diradical form of zethrene is destabilized by losing one aromatic sextet ring, but for heptazethrene ($y = 0.537$) and higher homologs (octazethrene, $y = 0.628$) it will be stabilized by recovery of one additional aromatic sextet ring and radical delocalization. Therefore, all the zethrene derivatives reported so far can be regarded as a regular closed-shell configuration, although, remarkable open-shell diradical character $y = 0.407$ was predicted by Nakano *et al.* for

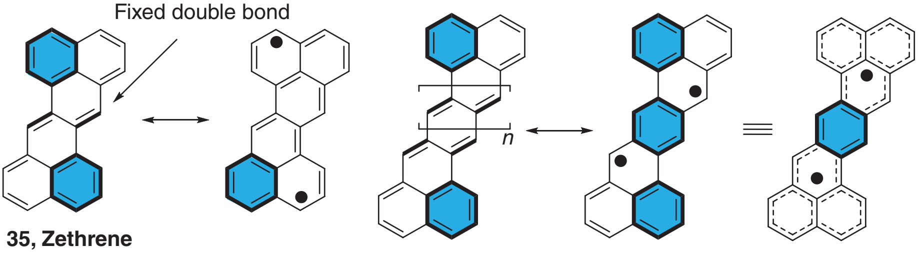

35, Zethrene

35a, *n* = 1: Heptazethrene
35b, *n* = 2: Octazethrene

Figure 1.6 Resonance structures of zethrene and higher order zethrenes.

zethrene based on occupancy numbers of spin-unrestricted Hartree–Fock natural orbitals (UNOs) [42].

The earlier reported zethrene compounds, by Clar, suffered from instability. Tobe and coworkers [43] and Wu *et al.* [44] had successfully developed reliable synthetic routes to stable zethrene compounds by blocking the most reactive 7,14-positions of zethrenes (Figure 1.7). Tobe's synthesis involved iodine-promoted transannular cyclization reaction from the tetradehydro[10]annulene precursor **36**, which gave the 7,14-diiodozethrene intermediate **37** that could be subjected to Sonogashira coupling reaction to yield 7,14-bis(phenylethynyl)zethrene **38**. Wu *et al.* constructed zethrene core by cyclodimerization of precursor 1-ethynyl-8-iodonaphthalenes **39** using catalytic palladium acetate. They reported up to 17 examples of zethrenes with a maximum yield of 73% obtained for the phenyl-substituted zethrene derivative **40**. At the same time, a new zethrene derivative with two biscarboximide groups located along the longer molecular axis **42** was synthesized by our group using Stille coupling between 4,6-dibromo-1,8-naphthalimide **41** and bis(tributylstannyl)acetylene followed by an *in situ* transannular cyclization reaction [45]. Further bromination at the 7,14-positions using *N*-bromosuccinimide (NBS) in *N.N*-dimethylformamide (DMF) was attempted on **42**. However, an oxidized product zethrenebis(dicarboximide)quinone **43** was obtained rather than the brominated product. The introduction of an electron-withdrawing group successfully enhanced the stability by lowering the HOMO energy level, and a 100 nm red shift in absorption spectrum was also observed. Very recently, Miao's group reported the synthesis of the parent zethrene **46**, which involved a Wittig reaction of bis(triphenylphosphonium) **44** with two paraformaldehydes leading to diene **45** followed by a Heck coupling in presence of excess palladium acetate [46]. Importantly, for the first time, the parent zethrene was explored as a hole-transporting material in OFETs with a field-effect mobility of up to $0.05\,\mathrm{cm^2\,V^{-1}\,s^{-1}}$. Other zethrene derivatives were also obtained by us and Tobe's group [47], but in contrast to the theoretical predictions, none of the known zethrenes displayed open-shell characteristics in the ground state.

Theoretical prediction of a larger diradical character in heptazethrene stimulated our group to synthesize the first relatively stable heptazethrene derivative heptazethrenebis(dicarboximide) **49** (Figure 1.8). This compound was synthesized by using a transannular cyclization approach involving simultaneous cyclization of an octadehydronaphthoannulene intermediate [48]. ^{1}H NMR observation showed a line broadening at room temperature due to the existence of thermally accessible triplet species and progressive line sharpening upon cooling due to the shift of the equilibrium to the singlet state. On the basis of DFT calculations, the energy of the singlet diradical state of **49** was located 5.8 and $7.9\,\mathrm{kcal\,mol^{-1}}$ lower than the closed-shell quinoidal state and open-shell triplet biradical state, respectively, thereby supporting an open-shell singlet diradical ground state, and the spin density was found to be homogeneously delocalized among the entire molecular backbone. A low electrochemical bandgap of 0.99 eV associated with lower energy UV–vis–NIR absorption band that likely originated from the admixing of the doubly excited electronic configuration (H,H-L,L) in

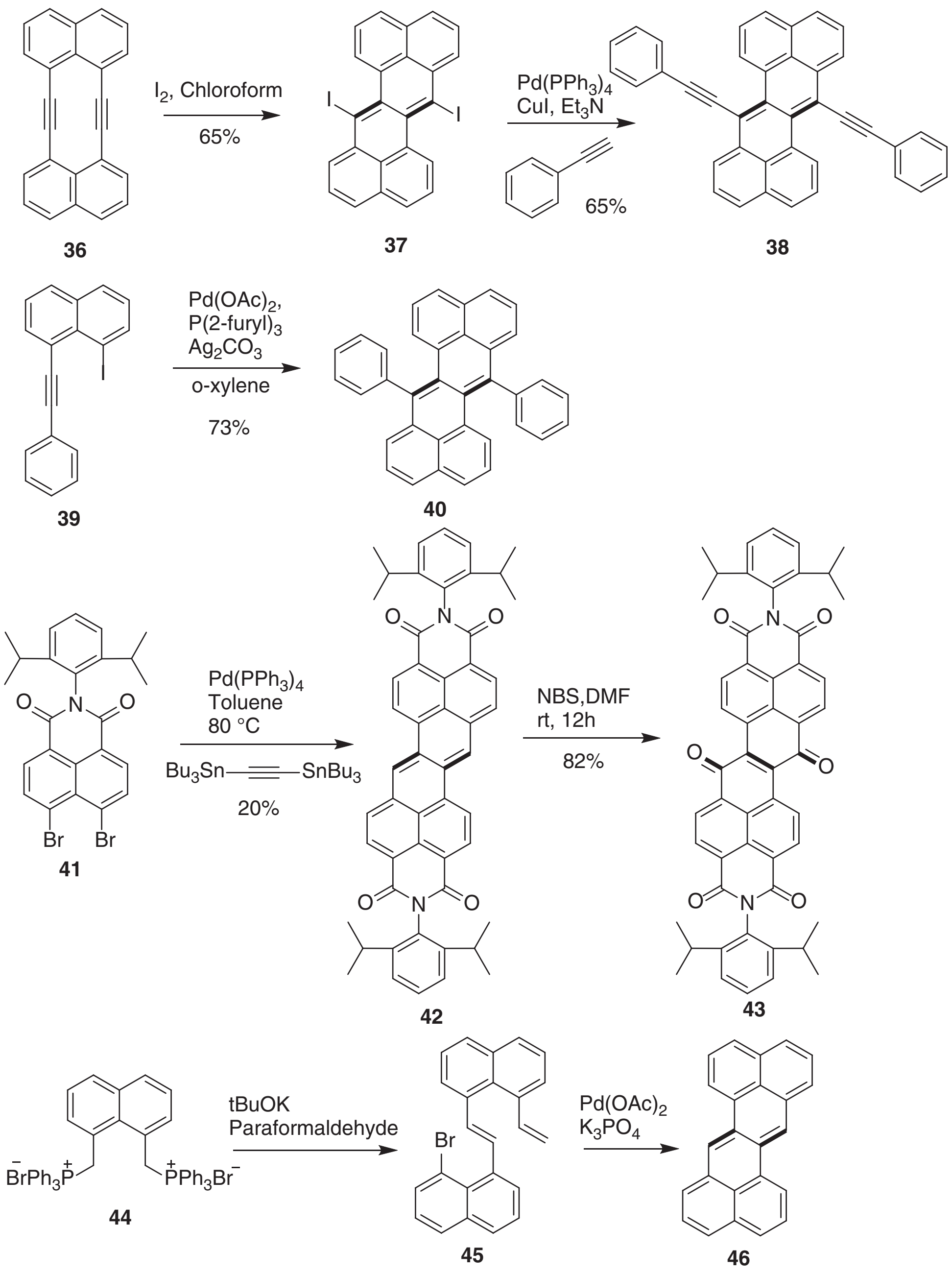

Figure 1.7 Synthesis of zethrene derivatives.

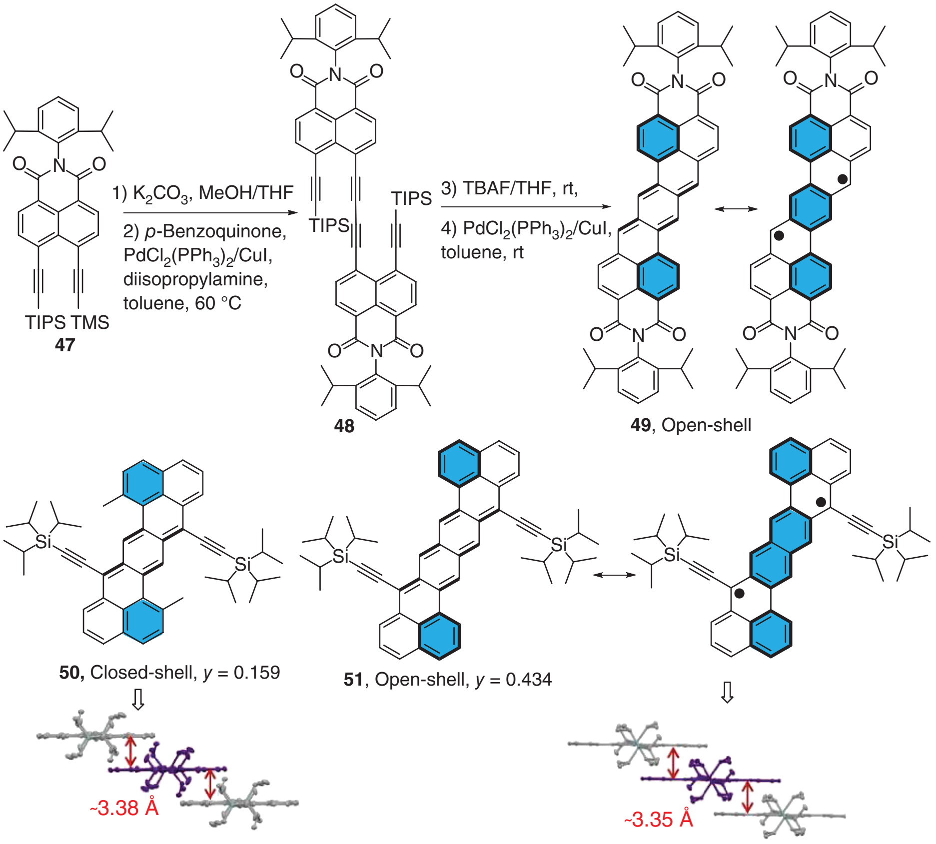

Figure 1.8 Heptazethrene and octazethrene derivatives. (Crystal figures are adapted with permission from Ref. [49]. Copyright 2012, American Chemical Society.)

the ground state further supports the open-shell character of **49**. Compound **49** showed reasonable photostability in solution; however, the material slowly decomposed during storage either as solution or in the solid state. In order to improve the stability without compromising the solubility, kinetic blocking at the most reactive radical sites is necessary. So, the next synthetic strategy to prepare heptazethrene-TIPS **50** and octazethrene-TIPS **51** was a nucleophilic addition of the corresponding diketone precursor with triisopropylsilylethynyl (TIPS)-magnesium chloride, followed by reduction with $SnCl_2$ (Figure 1.8) [49]. Compound **50** shows a typical p band similar to that of closed-shell PHs, while **51** displays an absorption pattern similar to that of **49**, indicating a probable open-shell character for **51**. The open-shell nature of **51** was further supported by the broadened ^{1}H NMR spectrum and the appearance of an ESR signal at room temperature due to presence of thermally excited triplet species as a consequence of a small singlet–triplet energy gap ($-3.87\ \mathrm{kcal\,mol^{-1}}$ based on SQUID measurement). Interestingly, although both **49** and **50** contain the same heptazethrene core, **50** showed the typical closed-shell feature unlike **49**. Calculations on **49** suggested a large delocalization of spins, which even extended to the imide groups, and the very low bandgap for **49** compared to that of **50** (1.46 eV) points out that the diradical character of heptazethrene is related not only to the recovery of aromatic sextets but also to the spin delocalization and the narrowing of the bandgap. Additionally, the diradical character of **51** is much larger than that of **50**, suggesting that the central naphthalene moiety could provide larger aromatic stabilization than a benzene moiety. Both **50** and **51** are packed into a 1D infinite chain via intermolecular π–π interactions, with an average π-stacking distance of 3.38 and 3.35 Å, respectively, which is larger than the intermolecular covalent π-bonding interaction seen in Kubo's bis(phenalenyl)-based diradicaloids.

Using a similar synthetic strategy, nucleophilic addition of TIPS-magnesium chloride to the corresponding diketone precursor **52** following reduction with tin chloride provided a dibenzoheptazethrene derivative **53**, which appeared to have an open-shell singlet diradical ground state (Figure 1.9). Another dibenzoheptazethrene isomer was also obtained using a different synthetic approach that involved a DDQ (2,3-dichloro-5,6-dicyano-1,4-benzoquinone)-mediated oxidative dehydrogenation of a dihydro precursor **54**, which was obtained by intramolecular cyclization of the corresponding diol promoted by $BF_3 \cdot OEt_2$. The ground state of both the molecules was systemically investigated by means of different experimental techniques assisted with DFT investigation. It was found that **53** possessed a larger diradical character (0.576) compared to isomeric **55** (0.309) [50]. This difference in diradical character between two isomeric structures was explained by the different number of aromatic sextet rings in the respective diradical resonance forms. Hence, in *benzenoid PHs with the same chemical composition, the molecule with more aromatic sextet rings in the diradical resonance forms exhibits greater diradical character.* This can be regarded an extension of Clar's aromatic sextet rule in the benzenoid PH-based singlet diradicaloids.

To further elaborate the fundamental structure–diradical character–physical property relationships in singlet diradicaloids the studies were conducted on homologous perylenes with different fusion modes and varied aromaticity. Therefore, two *p*-QDM bridged perylene dimers (**58** and **61**, Figure 1.10) were recently synthesized [51], in which the *p*-QDM subunit was fused with two perylene units either at both *peri*-positions of perylene monoimide (PMI) **58** or one at *peri*- and one at β-position of N-annulated-perylene (NP) **61**. A DDQ-mediated oxidative dehydrogenation approach was adopted to synthesize both **58** and **61** from their respective dihydro precursors **57** and **60**, which were obtained by intramolecular cyclization of the corresponding dimethoxy **56** and diol **59** derivatives promoted by $BF_3 \cdot OEt_2$. Interestingly, a different regioselectivity for the ring cyclization reaction was observed, which was attributed to (i) the activation of the β-position of electron-rich NP unit and (ii) formation of two five-membered rings rather than six-membered rings, which is thermodynamically more favorable. Similar to other quinoidal PHs, diradical resonance forms are supposed to contribute significantly to the ground states of both **58** and **61** due to the existence of the

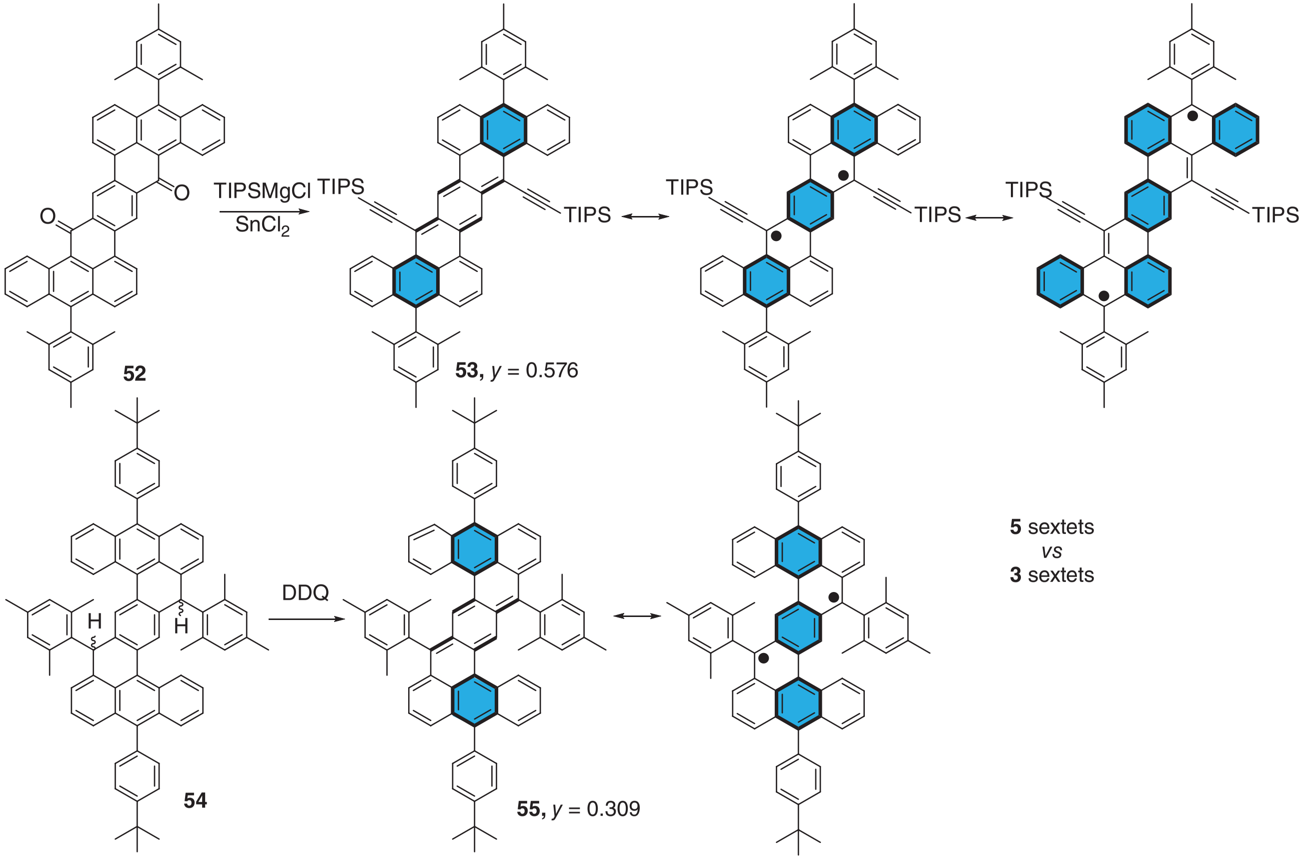

Figure 1.9 Exercise of Clar's sextet rule in isomeric dibenzoheptazethrene systems.

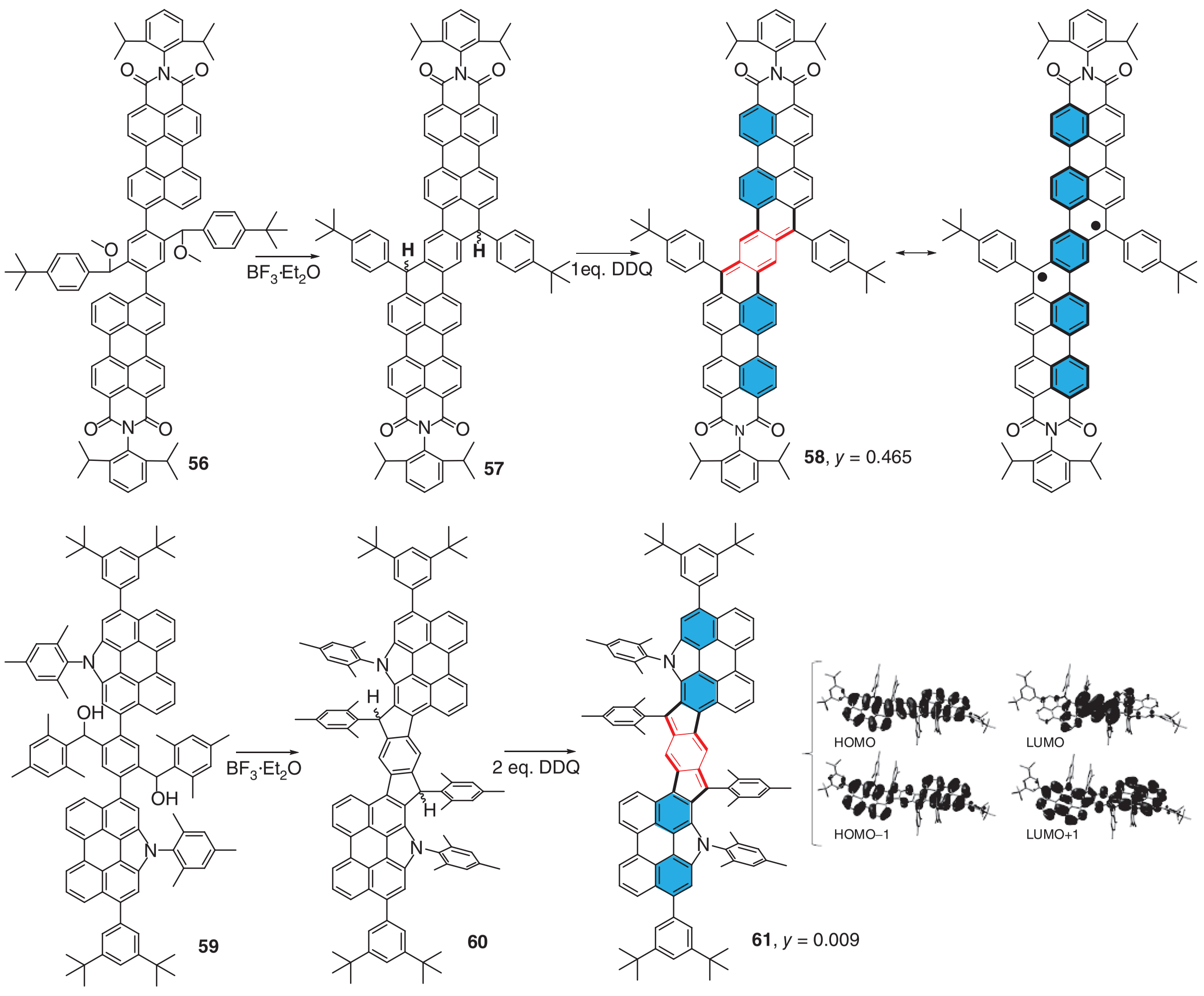

Figure 1.10 *p*-QDM bridged perylene dimers.

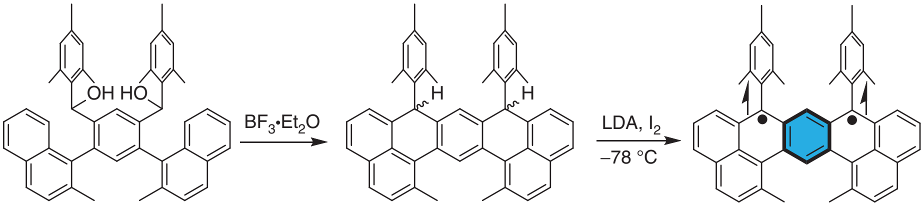

62 63 64

Figure 1.11 A persistent triplet biradical based on isomeric heptazethrene.

pro-aromatic *p*-QDM subunit which would help the recovery of one additional Clar's sextet ring. However, our systematic experimental and theoretical investigations revealed that compound **58** possesses an open-shell singlet diradical ground state ($\Delta E_{S-T} = -2.97$ kcal mol^{-1} from SQUID, and −3.3 kcal mol^{-1} from DFT), whereas compound **61** has a quinoidal closed-shell ground state, although the same number of Clar's aromatic sextets can be drawn in their respective diradical resonance forms. The singlet diradical character was theoretically estimated to be 0.465 for **58**, whereas the *s*-indacene bridged N-annulated-perylene dimer **61** was calculated to have negligible singlet diradical character ($y = 0.009$) with an obvious intramolecular charge transfer character (HOMO-1 to LUMO), which was evident from absorption spectra also. Compound **58** can be also regarded as an extended heptazethrene derivative.

Two naphthalene units when bridged by a *m*-xylylene moiety can only be drawn in an open-shell biradical form and no closed-shell resonance form exists (Figure 1.11). As a result, they are predicted to be highly reactive triplet biradicals. A kinetically blocked high-spin isomeric heptazethrene derivative (**64**) was synthesized by the deprotonation of **63**, obtained by $BF_3 \cdot OEt_2$-promoted intramolecular cyclization of the diol precursor **62**, with 2.5 equiv of lithium diisopropylamide (LDA) and subsequent oxidation by 1.06 equiv iodine in anhydrous 2-methyl tetrahydrofuran at −78 °C. This *in situ* generated biradical was confirmed to be a triplet biradical by ESR and electron spin transient nutation (ESTN) measurements and it was persistent at −78 °C under nitrogen protection for at least 1 day [52].

1.4
Anthenes and Periacenes

If two anthracene units are fused together by three single bonds between neighboring anthryls, it generates another type of extended molecular graphene called bisanthene (**65**) and longer homologs termed teranthene (**66**), quarteranthene (**67**), and so on (Figure 1.1). Related to anthenes are a kind of peri-fused acenes called periacenes, which can also be regarded as laterally extended perylenes. So far, no stable periacene other than bisanthene has been prepared. The major obstacle for the preparation of periacenes is their low stability, especially at the exposed zigzag edges. Even the closed-shell bisanthene is an unstable material [53]. Several strategies were developed in our group to stabilize the bisanthene, for example, by the introduction of imide groups onto the zigzag edges or by substitution at the meso positions with aryl or alkyne groups [54]. Notably, anthenes from teranthene onward will exhibit large singlet diradical character in the ground state, stemming from narrowed HOMO–LUMO energy gap and recovery of more aromatic sextet rings in the diradical resonance form, and the diradical character increases with more fused anthryl units. According to the DFT calculation, the singlet diradical character values are estimated to be 0.07 for bisanthene, 0.54 for teranthene, and 0.91 for quarteranthene (Figure 1.12) [55]. The diradical character of these molecules in terms of the energy balance between the formal loss of a double bond and the aromatic stabilization was well explained by Kubo and coworkers [56]. The aromatic stabilization energy of benzene, based on the homodesmic stabilization energy, is $\sim$90 kJ mol^{-1}, which is three times less than the C–C π-bond energy of $\sim$270 kJ mol^{-1}. Upon transformation to the diradical form, bisanthene **65** contains only two additional sextets; therefore, the destabilization energy due to the π-bond cleavage cannot be fully compensated, so electron pairing is favored in **65**, leading to a closed-shell ground state. In contrast, **66** and **67** both include three and four additional sextets, respectively, in their diradical resonance form; hence both the Kekulé and diradical forms should contribute to their ground state. Because the unpaired electrons are fixed to the meso positions of anthenes, the effect of delocalization is minimized and the discussion with regard to the diradical character can be focused on the aromatic stabilization effect. Therefore, anthenes represent excellent models to study how the formation of aromatic sextet rings affects diradical/polyradical characters in PHs with Kekulé-type structures and to investigate the spin-polarized state in zigzag-edged GNRs.

Bisanthene to quarteranthene derivatives have been prepared and isolated in the crystalline form by our group [54b] and Kubo's group [56], allowing a detailed investigation on their ground state molecular structure, chemical behavior, and physical properties. As shown in Figure 1.13, nucleophilic addition of the lithiated derivative of **68** to 1,5-dichloroanthraquinone **69** followed by reductive aromatization gave the teranthryl derivative **71**, which subsequently underwent

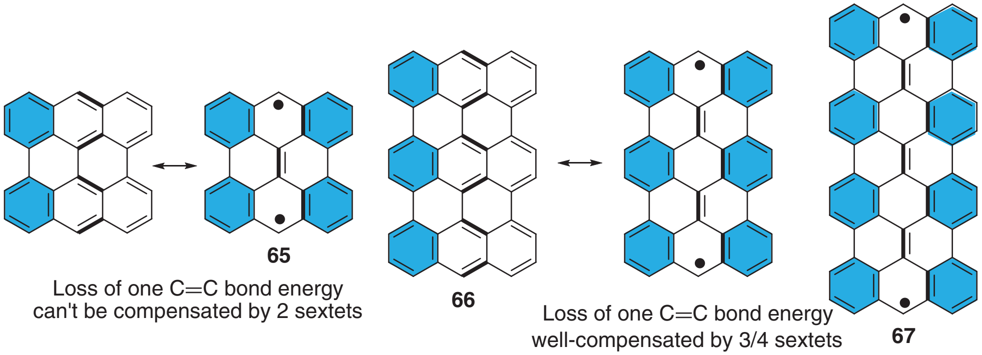

Figure 1.12 Structures of anthenes.

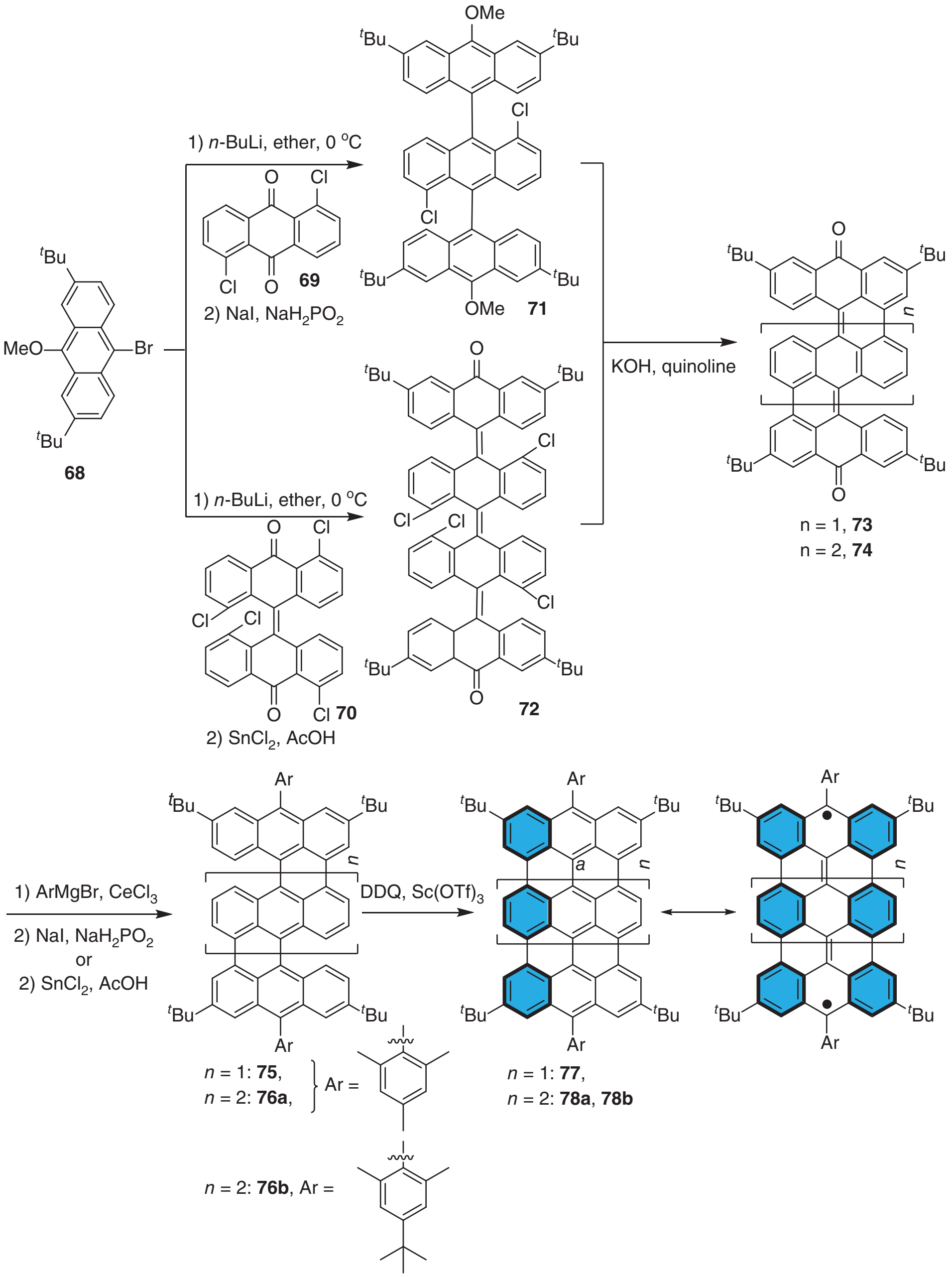

Figure 1.13 Syntheses of teranthene and quarteranthene derivatives.

cyclization and demethylation in a single step promoted by KOH/quinoline to afford the partially ring-fused quinone system **73**. Treatment of **73** with 2-mesitylmagnesium bromide in the presence of $CeCl_3$ and subsequent reductive aromatization with NaI/NaH_2PO_2 generated a partially cyclized hydrocarbon **75**. Cyclization of **75** promoted by $DDQ/Sc(OTf)_3$, followed by quenching the reaction with hydrazine hydrate, gave teranthene **77** as a dark-green solid. The quarteranthene was synthesized [55] using an identical synthetic approach. Lithiation of **68** followed by the coupling with (*Z*)-1,1′,5,5′-tetrachlorobianthrone **70** and treatment with $SnCl_2$ in acetic acid gave **72**, which underwent cyclization with KOH/quinoline to give a partially ring-closed quinone derivative **74**. Treatment of **74** with the respective arylmagnesium bromides in the presence of $CeCl_3$ and subsequent reductive aromatization with $SnCl_2$ in acetic acid afforded the partially ring-closed hydrocarbons **76a** and **76b**. Cyclization of **76a** and **76b** with $DDQ/Sc(OTf)_3$ followed by quenching with triethylamine/hydrazine hydrate gave the desired quarteranthenes **78a** and **78b**, respectively, as bluish-black solids.

Compound **77** exhibited moderate stability in solution with a half-life of around 3 days upon exposure to air at room temperature. Similar to phenalenyl-based open-shell PHs with singlet diradical ground state, the solution of **77** in CD_2Cl_2 showed no ^1H NMR signals from the teranthene core at room temperature, while progressive line sharpening was observed upon cooling, caused by the thermally excited triplet species due to a small singlet–triplet energy gap (1920 K by SQUID measurements). In contrast, the NMR baseline of **78a** remained flat even when the temperature was lowered to 183 K. The absence of NMR signals for **78a** accounts for the large population of thermally accessible triplet biradical species. The singlet–triplet energy gap for **78a** was determined to be 347 K by SQUID, which indicates that **78a** is easily activated to a triplet state with nearly 50% populated triplet species at room temperature. In contrast, the sharp ^1H NMR signals observed for bisanthene indicate that the influence of the triplet species is negligible owing to its much larger singlet–triplet gap (6810 K), resulting in a closed-shell ground state with negligible diradical contribution. The single-crystal data gave further information about the bond length alternation, as a bond in **78a** is 1.412 Å, much shorter than that in teranthene **77** (1.424 Å), which is considerably shorter than length of an sp^2 C–C single bond (1.467 Å) and the corresponding one in bisanthene (1.447 Å), resulting from the enforcement of diradical resonance contribution. In addition, the highest harmonic oscillator model of aromaticity (HOMA) values of outer six-membered rings in quarteranthene indicates more benzenoid character at the peripheral rings and, hence, a larger diradical character compared to bisanthene.

Perylene and bisanthenes can be regarded as periacenes as they have constant armchair edges and laterally growing zigzag edges. Experimentally, the synthesis of periacenes higher than bisanthene is challenging. Examples of higher order periacenes are peri fusion of tetracene leading to peritetracene **79** and peri fusion of pentacene resulting in peripentacene **80** (Figure 1.14). The chemical structure of periacenes, similar to that of anthenes, can be drawn as either a closed-shell Kekulé form or an open-shell diradical/tetraradical form. In both cases, more

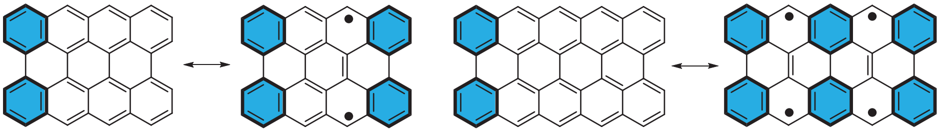

79
Peritetracene

80
Peripentacene

Figure 1.14 Structures of periacenes.

aromatic sextet rings would appear in the open-shell form than in the closed-shell form. The diradical character will increase with the increase in molecular size as a result of a narrowed bandgap. Theoretical calculations conducted by Jiang *et al.* pointed out a crossover from a nonmagnetic phase to an antiferromagnetic phase for both periacenes and anthenes starting from bisanthene onwards, and an open-shell ground state is therefore expected for these type of GNRs [57]. Synthesis of a peritetracene derivative is yet to be reported, and only one potential precursor, that is, monobromo-tetracene dicarboximide, was reported by our group [58]. The only experimental evidence of peripentacene was the mass spectroscopic peak of gas-phase disproportionation products [59]. Unfortunately, the preparation of periacenes longer than bisanthene has not been achieved yet, although some efforts have been devoted by our group and Müllen's group recently.

The synthetic approach involves the nucleophilic addition of TIPS lithium reagent to bispentacenequinone **82**, obtained from dimerization of pentacenyl monoketone **81**, followed by reductive aromatization with NaI/NaH_2PO_2 to afford the cruciform 6,6′-dipentacenyl **83** (Figure 1.15) [60]. Compound **83** exhibits two face-to-face π-stacking axes in a single crystal, which allows two-directional isotropic charge transport and field-effect mobilities of up to $0.11\,cm^2\,V^{-1}\,s^{-1}$, obtained on the basis of its vapor-deposited thin films. Further study was conducted by applying oxidative photocyclization of **82** to obtain partially fused bispentacenequinone **84** [61]. However, the subsequent nucleophilic reaction did not generate the desired 1,2-addition adduct. An unexpected 1,4-Michael addition product **85** was obtained when compound **84** was treated with excess of the Grignard reagent 1-bromo-3,5-di-*tert*-butylbenzene in anhydrous tetrahydrofuran (THF) followed by acidification in air, which was confirmed by X-ray crystallographic analysis. Further treatment of **85** with excess Grignard reagent followed by acidification in air gave the tetraaryl-substituted fused bispentacenequinone **86**. Single-crystal analysis revealed an α,β-unsaturated ketone structure in the fused bispentacenequinones **84** and **85**, which may account for the unusual Michael addition reactions.

The "pyrene approach" attempted by Müllen *et al.* involves the cyclization of tetracyano derivative **87** to afford the tetraketone **88**, which failed to undergo further photocyclization [62]. Adopting an alternative path by oxidative cyclodehydrogenation of **87** in presence of $PIFA/BF_3$ and subsequent acid-promoted acylation gave only trace amount of the target peripentacenetetraketone **89**, which showed very poor solubility, and no further reactions were conducted. It shows that periacenes beyond bisanthene is still a big challenge.

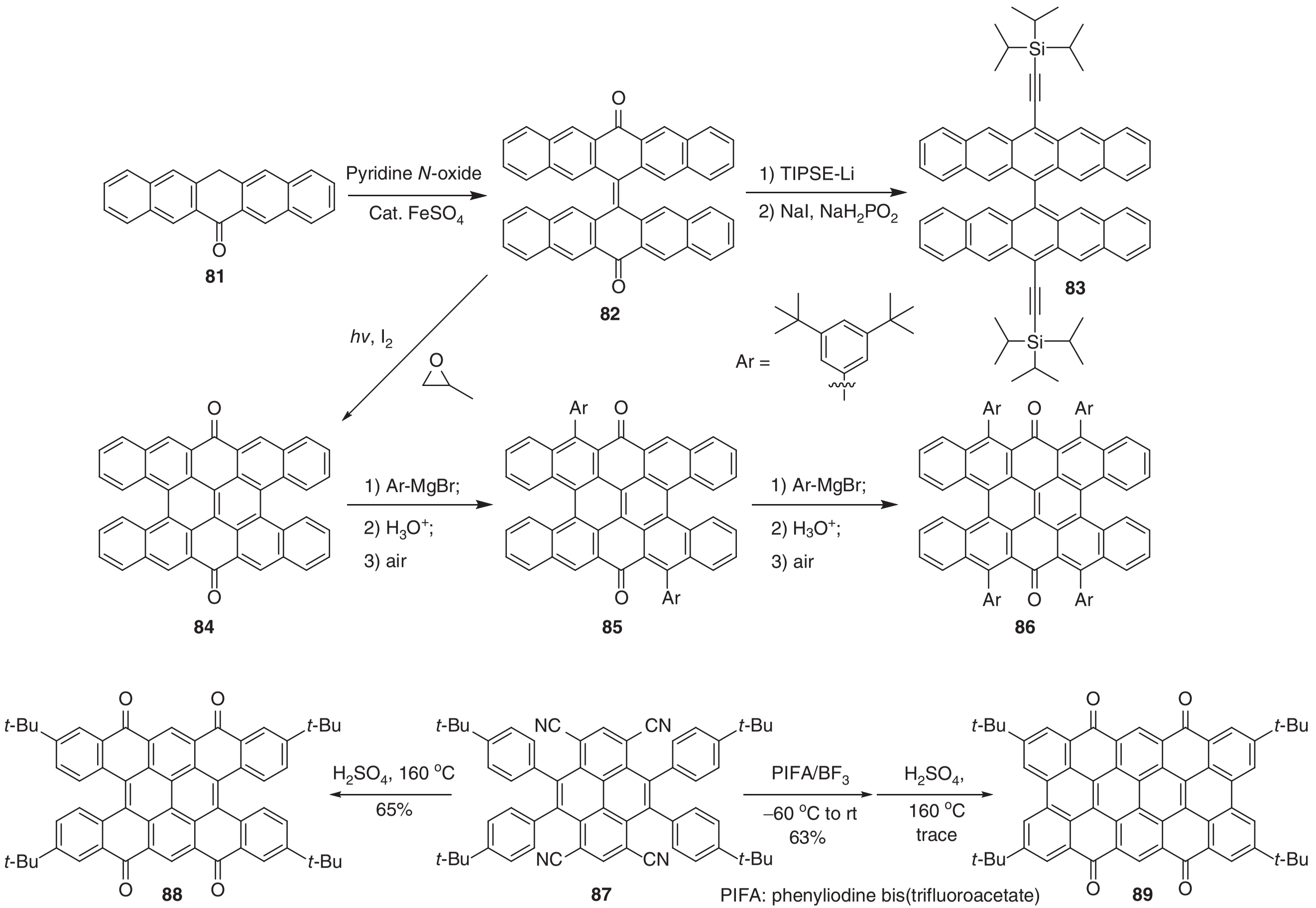

PIFA: phenyliodine bis(trifluoroacetate)

Figure 1.15 Preliminary studies toward the synthesis of peripentacene.

1.5
π-Extended *p*-Quinodimethane

The parent *para*-quinodimethane is a quinoidal structure that can be represented with a structural resonance between the quinoidal form and a diradical form with recovery of the Clar's sextet ring, which accounts for its higher reactivity. By terminal substitution at the methylene sites with four phenyl groups, a stable *p*-QDM derivative, Thiele's hydrocarbon, was obtained, which was reported to possess a quinoidal closed-shell ground state with a well-defined bond alternation in the *p*-QDM core (1.346 and 1.449 Å) according to single-crystal analysis. The crystallographic analysis of the extended *p*-QDM derivative (Tschitschibabin's hydrocarbon) revealed that the bond length in the central part lies halfway between the double-bond and single-bond values (1.420 and 1.372 Å), indicating significant contribution of the diradical resonance form to the ground state (Figure 1.16). Hence, the extension of *p*-QDM can generate another interesting π-scaffold with significant diradical character.

Electron-withdrawing cyano (CN) groups, at the terminal methylene sites (radical centers), are also usually employed to gain better stability for the extended *p*-QDM derivatives [63]. Our group's attempt to stabilize the Tschitschibabin's hydrocarbon involved benzannulation of the central biphenyl unit to generate the tetrabenzannulated hydrocarbons **91** and **93** (Figure 1.17), which should favor a closed-shell ground state (**91-C** and **93-C**), as two aromatic Clar's sextets are lost in their respective diradical resonance forms [64]. However, the closed-shell forms of **91** and **93** adopt a contorted geometry with a larger steric hindrance among the anthryl peri hydrogens, making the corresponding orthogonal diradical structures (**91-O** and **93-O**) more favorable. A thorough experimental investigation assisted with theoretical calculation supported a closed-shell quinoidal ground state for **91**, while **93** can be regarded as a weakly coupled triplet biradical in the ground state. The better thermodynamic stability of the diradical ground state in **93** can be credited to the efficient spin delocalization on the fluorenyl units. The 4-*tert*-butylphenyl-substituted compound **91** possesses a closed-shell ground state (i.e., **91-C**) and a diradical excited-state that was chemically obtained by the reduction of the diol precursor **90**, and the diradical excited-state gradually decayed to the closed-shell ground state **91-C** with a half-life time of 495 min overcoming the

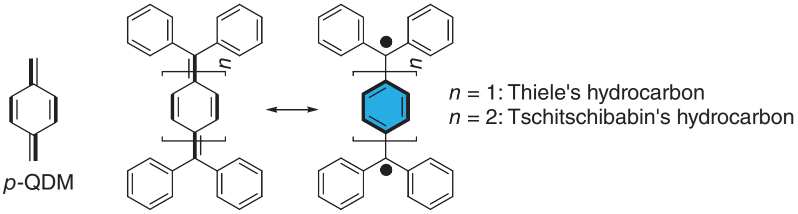

Figure 1.16 Parent *p*-QDM and its derivative.

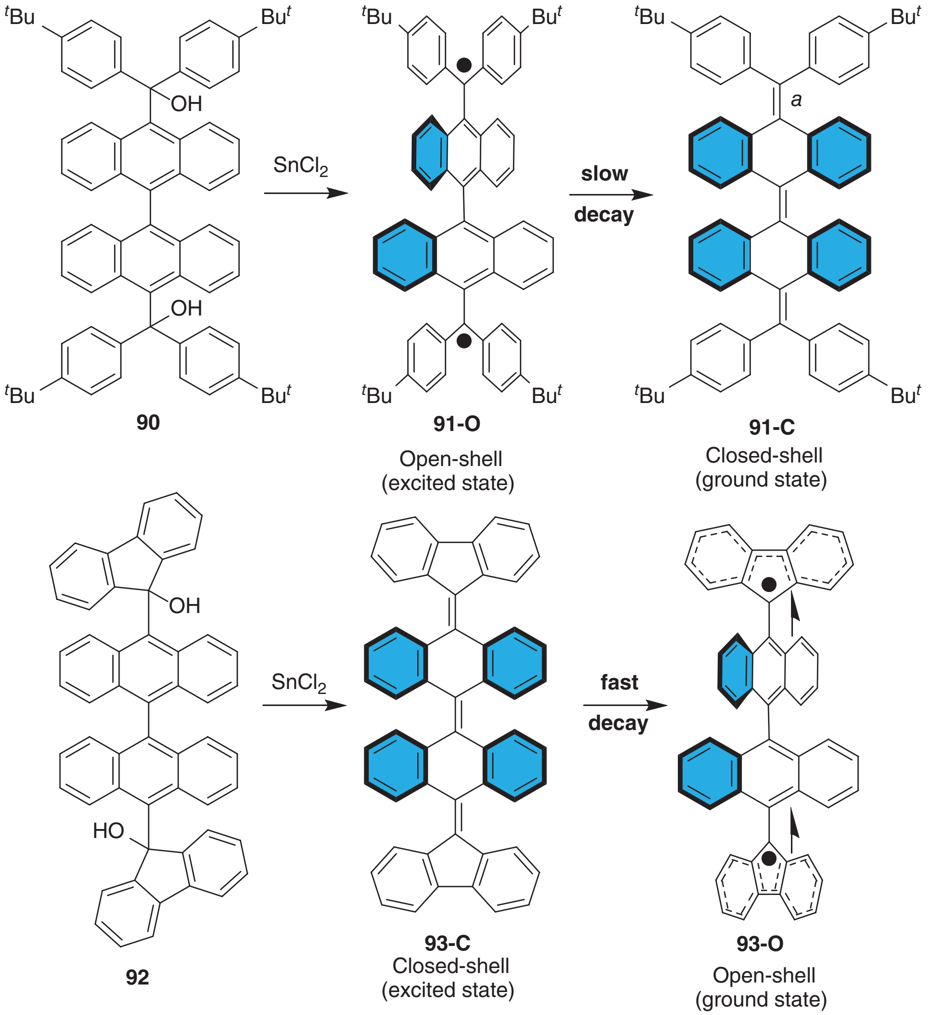

Figure 1.17 Tetrabenzo-Tschitschibabin's hydrocarbons.

large energy barrier (95 kJ mol^{-1}) for the transition from the orthogonal diradical form (**91-O**) to a butterfly-like quinoidal form (**91-C**). On the other hand, the triplet biradical ground state of **93** (i.e., **93-O**) was confirmed by the absence of any NMR signal and the presence of a strong ESR signal with a singlet–triplet energy gap of 1.4 kJ mol^{-1} as determined by SQUID measurements. An attempt to isolate the closed-shell form of **93** (i.e., **93-C**) failed, as the intermediate quickly relaxed back to the more stable biradical ground state.

These inspiring results stimulated our group to synthesize a series of tetracyano-oligo(N-annulated perylene)quinodimethanes from the corresponding dibromo derivatives **94** using Takahashi coupling and subsequent oxidation

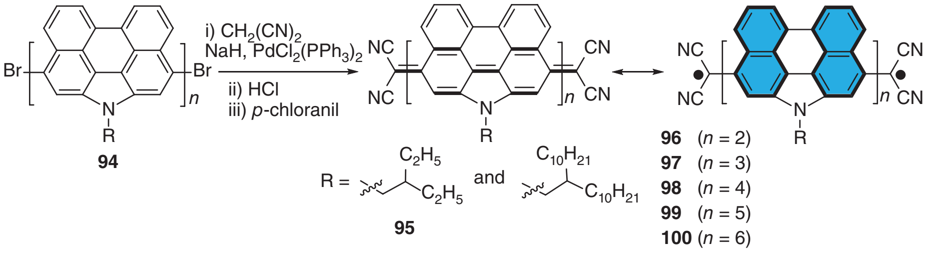

Figure 1.18 Tetracyano-N-annulated perylene quinodimethanes.

with *p*-chloranil [65]. These oligomers are regarded as more π-extended, benzannulated *p*-QDMs, and their stability and solubility were ensured by cyano- and *N*-alkyl- substitution, respectively (Figure 1.18). These oligomers exhibited an interesting chain-length dependence of their ground states, with a closed-shell **95** to open-shell singlet diradical for **96–98**, and then to a weakly coupled open-shell triplet biradical for **99** and **100**, as revealed by variable-temperature ESR spectroscopic measurements. The enhanced diradical character in the higher order oligomers can be mainly ascribed to the large steric repulsion between the neighboring perylene units causing a strain release from the rigid quinoidal structure to the more flexible diradical resonance form. In addition, the recovery of aromaticity of the quinoidal perylene units in the diradical form helps the longer oligomers to gain highest aromatization stability and hence the larger diradical character, approaching nearly 1 for the pentamer and hexamer. In fact, calculation showed that for the pentamer and hexamer the spins are largely distributed at the terminal perylene units, making them act like two separated radicals.

To minimize the influence of strain release, planarized tetracyanoquaterylenequinodimethane (**105**) and hexarylenequinodimethane (**106**) were prepared from the corresponding dibromo-rylenes **103** and **104** (Figure 1.19) [66]. In contrast to **96** with a large diradical character, the fused **105** has a closed-shell quinoidal ground state due to the efficient intramolecular antiferromagnetic coupling between the two spins via a double spin polarization mechanism. Compound **106** has a singlet diradical ground state due to the accumulated

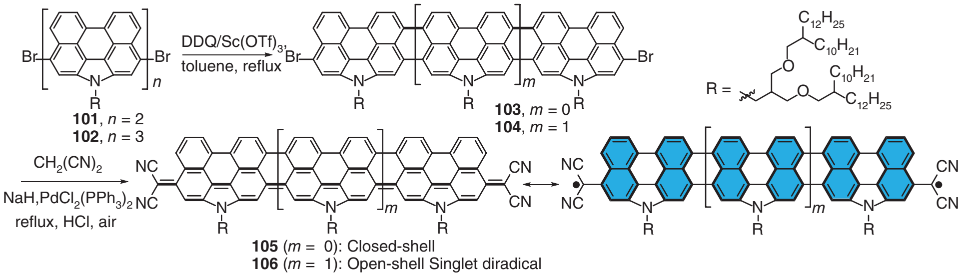

Figure 1.19 Fused tetracyano-N-annulated rylene quinodimethanes.

resonance energy via the formation of six aromatic naphthalene units in the diradical form. Nevertheless, the theoretical diradical character of **106** was found to be 0.064, which was quite small with larger singlet–triplet energy gap of −4.21 kcal mol^{-1}, compared to that of **97**. This comparison leads to a valuable conclusion that the dihedral angle between the rylene cores plays a critical role in fine-tuning the electronic configuration of quinoidal molecules.

In a recent report [67], our group showed that the incorporation of one thiophene unit between the rylene and the dicyanomethylene site in closed-shell **95** and **105** readily turns on their diradical states. A similar Takahashi reaction on **107** and **109** with malononitrile followed by oxidation in presence of *p*-chloranil (for **107**) and air (for **109**) afforded the respective desired compounds **108** and **110** (Figure 1.20). Both compounds have a singlet diradical ground state with diradical character estimated as 0.81 (for **108**) and 0.93 (for **110**) based on CASSCF(2,2)/6-31G calculations. The larger diradical contribution for **110** is in agreement with the stronger ESR signal and the small singlet–triplet energy gaps of −0.16 kcal mol^{-1} as compared to −4.71 kcal mol^{-1} for **108**, determined by SQUID measurements. Such a strong diradical contribution can be attributed to the recovery of two additional aromatic thiophene rings in the diradical resonance forms together with the conformational flexibility around the thiophene–rylene connections.

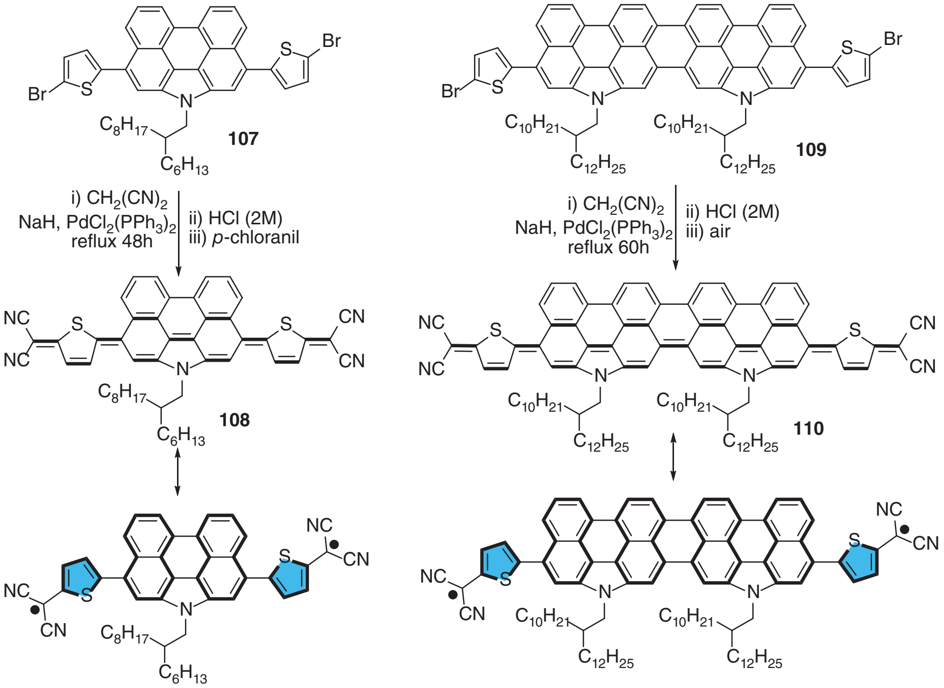

Figure 1.20 Tetracyanothiophene-capped N-annulated perylene quinodimethanes.

1.6
Triangulene-Based Triplet Biradicals

The C_3-symmetric higher order phenalenyl is called triangulene, which is regarded as the basic non-Kekulé polynuclear benzenoid compound with at least two carbon atoms not participating in the double-bond network, giving rise to an open-shell ground state. The first attempt to synthesize triangulene was made by Clar, but he obtained only the polymerized product because of its kinetic instability [68]. Theoretically, the higher reactivity can be explained by a triplet ground state for this system in the neutral state with large spin densities at the edge sites. A large SOMO–SOMO interaction in this triangulene system was predicted, leading to the formation of a π-stacked radical polymer with possible enhancement of the electron and hole mobilities compared with the phenalenyl monoradicals. Hence, triangulene could be a potential building block for thermo and photoresponsive conductive and magnetic materials [69, 70].

Nakasuji *et al.* attempted the synthesis of biradical species by treating the dihydrotriangulene **111** precursor with *p*-chloranil [71]. The strategy aimed to increase the kinetic stability of the phenalenyl radical by the introduction of bulky *tert*-butyl groups on three vertexes of the triangular triangulene system to minimize the electronic perturbation. Nevertheless, the triangulene system obtained was highly reactive. A variable-temperature ESR study was conducted to monitor the chemical oxidation step (Figure 1.21), and rapid freezing of the sample at intermediate stage gave a superposition of a doublet monoradical species and a fine-structure ESR spectrum of a typical triplet state which was

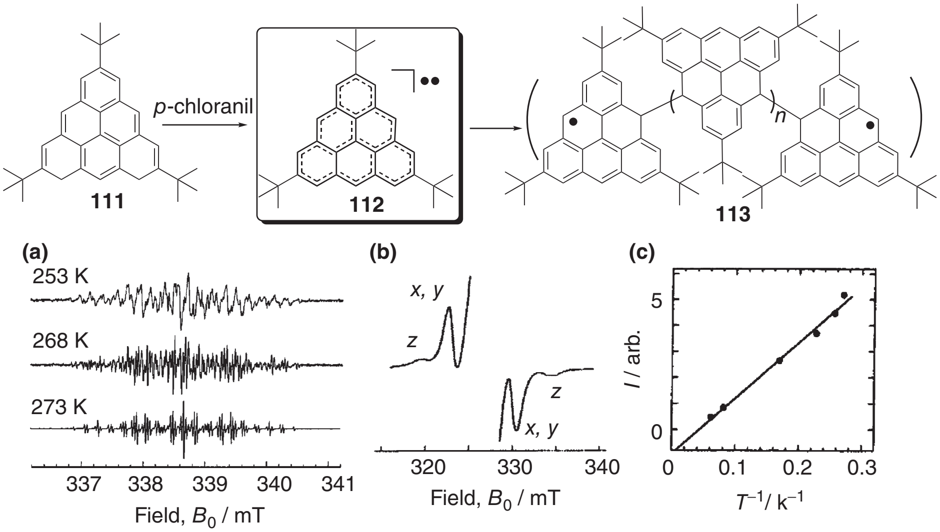

Figure 1.21 Synthetic route to tri-*tert*-butyl triangulene biradical **113** and its characterization by variable-temperature ESR spectroscopy. (Adapted with permission from Ref. [71]. Copyright 2001, American Chemical Society.)

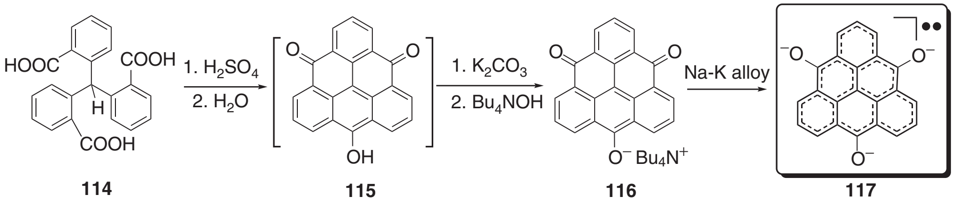

Figure 1.22 Synthesis of the biradical trianion **117**.

attributed to compound **113**, a true hydrocarbon with a threefold rotation axis (Figure 1.21b). The linear dependence of the triplet signal intensity I on T^{-1} (Figure 1.21c) showed that the triplet was the ground state, which corroborated the theoretical prediction.

The trioxytriangulene biradical is another type of novel open-shell compound with stable triplet ground state, as reported by Allinson *et al.* by reduction of the corresponding ketones (Figure 1.22). Similar to the phenalenyl system, substitution of oxygen atoms at the strategic positions of triangulene can make this system stable, and their electronic structures significantly differ from that of the parent triangulene [72]. The biradical trianion species **117** was remarkably stable in degassed solution at room temperature because of the extension of delocalization and protection from dimerization [73]. ESR investigation determined a triplet ground state for **117**, whereas the unsymmetric derivatives appeared to be ESR silent with a singlet ground state [74]. The introduction of heteroatoms was believed to lift the degeneracy of the nonbonding molecular orbitals, causing a kinetic exchange interaction that dominated over dynamic spin polarization in the parent π systems.

1.7
Potential Applications

Open-shell singlet diradical PHs are quite unique by nature, as they show promising optical, electronic, and magnetic properties compared to their closed-shell counterparts. A good example was reported by Kamada *et al.* [75] in which large TPA cross-section values of 424 ± 64 GM at 1425 nm for **28d** and 890 ± 130 GM at 1500 nm for **29a** were reported, which are comparable to similar sized donor–acceptor type TPA chromophores. Our open-shell systems are also being investigated as potential TPA chromophores. Indeed, larger TPA cross sections were observed for **51** (1200 GM), **53** (2800 GM), and **58** (1300 GM) compared to closed-shell **50** (920 GM), **55** (530 GM), or **61** (590 GM) with smaller diradical character [76]. Closed-shell **105**, open-shell **106** (Figure 1.19), and both compounds **108** and **110** (Figure 1.20) showed large TPA cross sections by Z-scan measurements. Our study on the oligomers with a moderate diradical character (**96**, Figure 1.18) showed higher TPA cross sections than those with large diradical characters (e.g., **98–100**, Figure 1.18), which is in agreement with theoretical predictions that suggest that the second-hyperpolarizability (a quantity related to the TPA cross section) is the highest for systems with moderate singlet diradical character, thus opening the possibilities for nonlinear optical applications [42, 75].

A singlet diradical compound **28d**, relying on its long-range covalent bonding interactions, showed electroconductivity of 1.0×10^{-5} S cm^{-1} out of a compressed pellet at room temperature [77]. Compound **28d** was reported to exhibit balanced charge-transport characteristics for both electrons and holes on the order of 10^{-3} cm^2 V^{-1} s^{-1} [78]. Lately, it has been found that chromophores with a small singlet diradical character could exhibit a unique singlet fission phenomenon, which has shown promise for potential applications in next-generation organic photovoltaic devices [79]. The unique magnetic activity upon external stimuli (e.g., heat, light, electric field, magnetic field, etc.) qualifies them as multifunctional responsive materials and as spin injection/transporting materials in spintronic devices [80].

1.8
Conclusion

Even though open-shell systems had shown promise for materials science applications, stability issues of such systems had to be overcome. Because of the high reactivity of radicals, most open-shell species have a tendency to be short-lived, which largely hinder their practical applications. The major reasons for this instability are intermolecular dimerization and oxidation. Recent advancements by several groups, including ours, have resulted in some realistic approaches to prepare stable diradicaloids with adequate stability comparable to other closed-shell π-conjugated systems. The progress on thermodynamically stable diradical compounds has addressed several methods in solving stability problems, including (i) delocalization of radicals in the π backbone, (ii) attachment of bulky groups at the most reactive site, (iii) attachment of electron-withdrawing substituents at strategic positions, and (iv) aromatic stabilization. Hence, Clar's aromatic sextet rule also can be further extended to the open-shell, singlet diradicaloid PHs. We feel that such stabilization approach can make feasible future targets that can be extended from diradical to high-spin polyradical systems for device-based applications at the nanoscale, and even at the molecular scale.

References

1. Wu, J., Pisula, W., and Müllen, K. (2007) *Chem. Rev.*, **107**, 718–747.
2. Clar, E. (1972) *The Aromatic Sextet*, Wiley-VCH Verlag GmbH, London.
3. Bendikov, M., Duong, H.M., Starkey, K., Houk, K.N., Carter, E.A., and Wudl, F. (2004) *J. Am. Chem. Soc.*, **126**, 7416–7417.
4. (a) Abe, M. (2013) *Chem. Rev.*, **113**, 7011–7088; (b) Sun, Z., Ye, Q., Chi, C., and Wu, J. (2012) *Chem. Soc. Rev.*, **41**, 7857–7889; (c) Sun, Z., Zeng, Z., and Wu, J. (2013) *Chem. Asian J.*, **8**, 2894–2904.
5. Morita, Y. and Nishida, S. (2010) in *Stable Radicals: Fundamentals and Applied*

Aspects of Odd-Electron Compounds (ed R.G. Hicks), John Wiley & Sons, Inc, pp. 81–145.

6. Kubo, T. (2014) *Chem. Rec.*, **15**, 218–232.
7. Noodleman, L. (1981) *J. Chem. Phys.*, **74**, 5737–5743.
8. Döhnert, D. and Koutecký, J. (1980) *J. Am. Chem. Soc.*, **102**, 1789–1796.
9. Yamaguchi, K. (1975) *Chem. Phys. Lett.*, **33**, 330–335.
10. Kamada, K., Ohta, K., Shimizu, A., Kubo, T., Kishi, R., Takahashi, H., Botek, E., Champagne, B., and Nakano, M. (2010) *J. Phys. Chem. Lett.*, **1**, 937–940.
11. Cheng, Y.C., Silbey, R.J., Da Silva Filho, D.A., Calbert, J.P., Cornil, J., and Brédas, J.L. (2003) *J. Chem. Phys.*, **118**, 3764.
12. (a) Bendikov, M., Wudl, F., and Perepichka, D.F. (2004) *Chem. Rev.*, **104**, 4891–4945; (b) Anthony, J.E. (2006) *Chem. Rev.*, **106**, 5028–5048; (c) Anthony, J.E. (2008) *Angew. Chem. Int. Ed.*, **47**, 452–483.
13. (a) Reddy, A.R. and Bendikov, M. (2006) *Chem. Commun.*, 1179–1181; (b) Reddy, A.R., Fridman-Marueli, G., and Bendikov, M. (2007) *J. Org. Chem.*, **72**, 51–61.
14. (a) Zade, S.S., Zamoshchik, N., Reddy, A.R., Fridman-Marueli, G., Sheberla, D., and Bendikov, M. (2011) *J. Am. Chem. Soc.*, **133**, 10803; (b) Zade, S.S. and Bendikov, M. (2012) *J. Phys. Org. Chem.*, **25**, 452–461.
15. Angliker, H., Rommel, E., and Wirz, J. (1982) *Chem. Phys. Lett.*, **87**, 208.
16. Houk, K.N., Lee, P.S., and Nendel, M. (2001) *J. Org. Chem.*, **66**, 5517.
17. Hachmann, J., Dorando, J.J., Avilés, M., and Chan, G.K.-L. (2007) *J. Chem. Phys.*, **127**, 134309.
18. Jiang, D. and Dai, S. (2008) *J. Phys. Chem. A*, **112**, 332–335.
19. Qu, Z., Zhang, D., Liu, C., and Jiang, Y. (2009) *J. Phys. Chem. A*, **113**,7909–7914.
20. Ishidaa, T. and Aihara, J. (2009) *Phys. Chem. Chem. Phys.*, **11**, 7197.
21. Purushothaman, B., Parkin, S.R., and Anthony, J.E. (2010) *Org. Lett.*, **12**, 2060.
22. (a) Zade, S.S. and Bendikov, M. (2010) *Angew. Chem. Int. Ed.*, **49**, 4012–4015; (b) Ye, Q. and Chi, C. (2014) *Chem. Mater.*, **26**, 4046.
23. Watanabe, M., Chang, Y.J., Liu, S.-W., Chao, T.-H., Goto, K., Islam, M.M., Yuan, C.-H., Tao, Y.-T., Shinmyozu, T., and Chow, T.J. (2012) *Nat. Chem.*, **4**, 574–578.
24. Tönshoff, C. and Bettinger, H.F. (2010) *Angew. Chem. Int. Ed.*, **49**, 4125–4128.
25. Kaur, I., Jazdzyk, M., Stein, N.N., Prusevich, P., and Miller, G.P. (2010) *J. Am. Chem. Soc.*, **132**, 1261–1263.
26. Gao, X., Hodgson, J.L., Jiang, D., Zhang, S.B., Nagase, S., Miller, G.P., and Chen, Z. (2011) *Org. Lett.*, **13**, 3316–3319.
27. Purushothaman, B., Bruzek, M., Parkin, S.R., Miller, A.-F., and Anthony, J.E. (2011) *Angew. Chem. Int. Ed.*, **50**, 7013.
28. Haddon, R.C. (1975) *Nature*, **256**, 394–396.
29. Enoki, T., Kobayashi, Y., and Fukui, K. (2007) *Int. Rev. Phys. Chem.*, **26**, 609–645.
30. Nakasuji, K. and Kubo, T. (2004) *Bull. Chem. Soc. Jpn.*, **77**, 1791–1801.
31. Nakasuji, K., Yoshida, K., and Murata, I. (1983) *J. Am. Chem. Soc.*, **105**, 5136–5137.
32. (a) Murata, I., Sasaki, S., Klabunde, K.U., Toyoda, J., and Nakasuji, K. (1991) *Angew. Chem., Int. Ed. Engl.*, **30**, 172–173; (b) Ohashi, K., Kubo, T., Masui, T., Yamamoto, K., Nakasuji, K., Takui, T., Kai, Y., and Murata, I. (1998) *J. Am. Chem. Soc.*, **120**, 2018–2027.
33. Kubo, T., Shimizu, A., Sakamoto, M., Uruichi, M., Yakushi, K., Nakano, M., Shiomi, D., Sato, K., Takui, T., Morita, Y., and Nakasuji, K. (2005) *Angew. Chem. Int. Ed.*, **44**, 6564–6568.
34. Kubo, T., Shimizu, A., Uruichi, M., Yakushi, K., Nakano, M., Shiomi, D., Sato, K., Takui, T., Morita, Y., and Nakasuji, K. (2007) *Org. Lett.*, **9**, 81–84.
35. Shimizu, A., Hirao, Y., Matsumoto, K., Kurata, H., Kubo, T., Uruichi, M., and Yakushi, K. (2012) *Chem. Commun.*, **48**, 5629.
36. Kubo, T., Sakamoto, M., Akabane, M., Fujiwara, Y., Yamamoto, K., Akita, M., Inoue, K., Takui, T., and Nakasuji, K. (2004) *Angew. Chem. Int. Ed.*, **43**, 6474–6479.

37. Kubo, T., Yamamoto, K., Nakasuji, K., and Takui, T. (2001) *Tetrahedron Lett.*, **42**, 7997–8001.

38. Kubo, T., Sakamoto, M., and Nakasuji, K. (2005) *Polyhedron*, **24**, 2522–2527.

39. Kubo, T., Katada, Y., Shimizu, A., Hirao, Y., Sato, K., Takui, T., Uruichi, M., Yakushi, K., and Haddon, R.C. (2011) *J. Am. Chem. Soc.*, **133**, 14240–14243.

40. (a) Kubo, T., Yamamoto, K., Nakasuji, K., Takui, T., and Murata, I. (1996) *Angew. Chem., Int. Ed. Engl.*, **35**, 439; (b) Kubo, T., Yamamoto, K., Nakasuji, K., Takui, T., and Murata, I. (2001) *Bull. Chem. Soc. Jpn.*, **74**, 1999.

41. Clar, E., Lang, K.F., and Schulz-Kiesow, H. (1955) *Chem. Ber.*, **88**, 1520–1527.

42. Nakano, M., Kishi, R., Takebe, A., Nate, M., Takahashi, H., Kubo, T., Kamada, K., Ohta, K., Champagne, B., and Botek, E. (2007) *Comput. Lett.*, **3**, 333–338.

43. Umeda, R., Hibi, D., Miki, K., and Tobe, Y. (2009) *Org. Lett.*, **11**, 4104–4106.

44. Wu, T.C., Chen, C.H., Hibi, D., Shimizu, A., Tobe, Y., and Wu, Y.T. (2010) *Angew. Chem. Int. Ed.*, **49**, 7059–7062.

45. Sun, Z., Huang, K.W., and Wu, J. (2010) *Org. Lett.*, **12**, 4690–4693.

46. Shan, L., Liang, Z.-X., Xu, X.-M., Tang, Q., and Miao, Q. (2013) *Chem. Sci.*, **4**, 3294–3297.

47. (a) Sun, Z. and Wu, J. (2013) *J. Org. Chem.*, **78**, 9032–9040; (b) Hibi, D., Kitabayashi, K., Shimizu, A., Umeda, R., and Tobe, Y. (2013) *Org. Biomol. Chem.*, **11**, 8256–8261.

48. Sun, Z., Huang, K.-W., and Wu, J. (2011) *J. Am. Chem. Soc.*, **133**, 11896–11899.

49. Li, Y., Heng, W.-K., Lee, B.S., Aratani, N., Zafra, J.L., Bao, N., Lee, R., Sung, Y.M., Sun, Z., Huang, K.-W., Webster, R.D., López Navarrete, J.T., Kim, D., Osuka, A., Casado, J., Ding, J., and Wu, J. (2012) *J. Am. Chem. Soc.*, **134**, 14913–14922.

50. Sun, Z., Lee, S., Park, K., Zhu, X., Zhang, W., Zheng, B., Hu, P., Zeng, Z., Das, S., Li, Y., Chi, C., Li, R., Huang, K., Ding, J., Kim, D., and Wu, J. (2013) *J. Am. Chem. Soc.*, **135**, 18229–18236.

51. Das, S., Lee, S., Son, M., Zhu, X., Zhang, W., Zheng, B., Hu, P., Zeng, Z., Sun, Z., Zeng, Z., Li, R.-W., Huang, K., Ding, J., Kim, D., and Wu, J. (2014) *Chem. Eur. J.*, **20**, 11410–11420.

52. Li, Y., Huang, K.-W., Sun, Z., Webster, R.D., Zeng, Z., Zeng, W., Chi, C., Furukawa, K., and Wu, J. (2014) *Chem. Sci.*, **5**, 1908–1914.

53. Clar, E. (1948) *Chem. Ber.*, **81**, 52–63.

54. (a) Yao, J.H., Chi, C., Wu, J., and Loh, K.P. (2009) *Chem. Eur. J.*, **15**, 9299–9302; (b) Li, J., Zhang, K., Zhang, X., Chi, C., and Wu, J. (2010) *J. Org. Chem.*, **75**, 856–863; (c) Zhang, K., Huang, K., Li, J., Chi, C., and Wu, J. (2009) *Org. Lett.*, **11**, 4854–4857.

55. Konishi, A., Hirao, Y., Matsumoto, K., Kurata, H., Kishi, R., Shigeta, Y., Nakano, M., Tokunaga, K., Kamada, K., and Kubo, T. (2013) *J. Am. Chem. Soc.*, **135**, 1430–1437.

56. (a) Konishi, A., Hirao, Y., Nakano, M., Shimizu, A., Botek, E., Champagne, B., Shiomi, D., Sato, K., Takui, T., Matsumoto, K., Kurata, H., and Kubo, T. (2010) *J. Am. Chem. Soc.*, **132**, 11021–11023; (b) Hirao, Y., Konishi, A., Matsumoto, K., Kurata, H., and Kubo, T. (2012) *AIP Conf. Proc.*, **1504**, 863–866.

57. Jiang, D., Sumpter, B.G., and Dai, S. (2007) *J. Chem. Phys.*, **127**, 124703.

58. Yin, J., Zhang, K., Jiao, C., Li, J., Chi, C., and Wu, J. (2010) *Tetrahedron Lett.*, **51**, 6313–6315.

59. Roberson, L.B., Kowalik, J., Tolbert, L.M., Kloc, C., Zeis, R., Chi, X., Fleming, R., and Wilkins, C. (2005) *J. Am. Chem. Soc.*, **127**, 3069–3075.

60. Zhang, X., Jiang, X., Luo, J., Chi, C., Chen, H., and Wu, J. (2010) *Chem. Eur. J.*, **16**, 464–468.

61. Zhang, X., Li, J., Qu, H., Chi, C., and Wu, J. (2010) *Org. Lett.*, **12**, 3946–3949.

62. Zöphel, L., Berger, R., Gao, P., Enkelmann, V., Baumgarten, M., Wagner, M., and Müllen, K. (2013) *Chem. Eur. J.*, **19**, 17821–17826.

63. Zhu, X., Tsuji, H., Nakabayashi, K., Ohkoshi, S.-I., and Nakamura, E. (2011) *J. Am. Chem. Soc.*, **133**, 16342.

64. Zeng, Z., Sung, Y.M., Bao, N., Tan, D., Lee, R., Zafra, J.L., Lee, B.S., Ishida, M., Ding, J., López Navarrete, J.T., Li, Y., Zeng, W., Kim, D., Huang, K.-W., Webster, R.D., Casado, J., and Wu, J. (2012) *J. Am. Chem. Soc.*, **134**, 14513–14525.

65. Zeng, Z., Ishida, M., Zafra, J.L., Zhu, X., Sung, Y.M., Bao, N., Webster, R.D., Lee, B.S., Li, R.-W., Zeng, W., Li, Y., Chi, C., López Navarrete, J.T., Ding, J., Casado, J., Kim, D., and Wu, J. (2013) *J. Am. Chem. Soc.*, **135**, 6363–6371.

66. Zeng, Z., Lee, S., Zafra, J.L., Ishida, M., Zhu, X., Sun, Z., Ni, Y., Webster, R.D., Li, R.-W., López Navarrete, J.T., Chi, C., Ding, J., Casado, J., Kim, D., and Wu, J. (2013) *Angew. Chem. Int. Ed.*, **52**, 8561–8565.

67. Zeng, Z., Lee, S., Zafra, J.L., Ishida, M., Bao, N., Webster, R.D., López Navarrete, J.T., Ding, J., Casado, J., Kim, D., and Wu, J. (2014) *Chem. Sci.*, **5**, 3072–3080.

68. Clar, E. and Stewart, D.G. (1953) *J. Am. Chem. Soc.*, **75**, 2667–2672.

69. Morita, Y., Suzuki, S., Sato, K., and Takui, T. (2011) *Nat. Chem.*, **3**, 197–204.

70. Fukui, K., Inoue, J., Kubo, T., Nakazawa, S., Aoki, T., Morita, Y., Yamamoto, K., Sato, K., Shiomi, D., Nakasuji, K., and Takui, T. (2001) *Synth. Met.*, **121**, 1824–1825.

71. Inoue, J., Fukui, K., Kubo, T., Nakazawa, S., Sato, K., Shiomi, D., Morita, Y., Yamamoto, K., Takui, T., and Nakasuji, K. (2001) *J. Am. Chem. Soc.*, **123**, 12702–12703.

72. Allinson, G., Bushby, R.G., and Paillaud, J.L. (1993) *J. Am. Chem. Soc.*, **115**, 2062–2064.

73. Allinson, G., Bushby, R.G., Paillaud, J.L., and Thornton-Pett, M. (1995) *J. Chem. Soc., Perkin Trans.*, 385–390.

74. Allinson, G., Bushby, R.G., Jesudason, M.V., Thornton-Pett, M., and Taylor, M. (1997) *J. Chem. Soc., Perkin Trans. 2*, 147–156.

75. Kamada, K., Ohta, K., Kubo, T., Shimizu, A., Morita, Y., Nakasuji, K., Kishi, R., Ohta, S., Furukawa, S., Takahashi, H., and Nakano, M. (2007) *Angew. Chem. Int. Ed.*, **46**, 3544–3546.

76. Sun, Z., Zeng, Z., and Wu, J. (2014) *Acc. Chem. Res.*, **47**, 2582–2591.

77. Koike, H., Kubo, T., Uchida, K., Chikamatsu, M., Azumi, R., Mase, K., and Kanai, K. (2013) *Appl. Phys. Lett.*, **102**, 134103.

78. Chikamatsu, M., Mikami, T., Chisaka, J., Yoshida, Y., Azumi, R., and Yase, K. (2007) *Appl. Phys. Lett.*, **91**, 043506.

79. Smith, M.B. and Michl, J. (2010) *Chem. Rev.*, **110**, 6891–6936.

80. (a) Son, Y.W., Cohen, M.L., and Louie, S.G. (2006) *Phys. Rev. Lett.*, **97**, 216803; (b) Kim, W.Y. and Kim, K.S. (2008) *Nat. Nanotechnol.*, **3**, 408–412.